

**ASSESSMENT OF HYDROLOGIC  
TRANSPORT OF RADIONUCLIDES FROM  
THE GNOME UNDERGROUND NUCLEAR TEST SITE,  
NEW MEXICO**

*prepared by*

Sam Earman, Jenny Chapman,  
Karl Pohlmann and Roko Andricevic

**RECEIVED**  
**MAR 03 1997**  
**OSTI**

*submitted to*

Nevada Operations Office  
U.S. Department of Energy

**MASTER**

September 1996

**DISTRIBUTION OF THIS DOCUMENT IS UNLIMITED**

*✓*

**Publication No. 45143**

**DISCLAIMER**

**Portions of this document may be illegible  
in electronic image products. Images are  
produced from the best available original  
document.**

**ASSESSMENT OF HYDROLOGIC  
TRANSPORT OF RADIONUCLIDES FROM  
THE GNOME UNDERGROUND NUCLEAR TEST SITE,  
NEW MEXICO**

*prepared by*

Sam Earman, Jenny Chapman, Karl Pohlmann and Roko Andricevic  
Water Resources Center  
Desert Research Institute  
University and Community College System of Nevada

Publication No. 45143

*submitted to*

Nevada Operations Office  
U.S. Department of Energy  
Las Vegas, Nevada

September 1996

---

The work upon which this report is based was supported by the U.S. Department of Energy under Contract #DE-AC08-95NV11508.

## ABSTRACT

The U.S. Department of Energy (DOE) is operating an environmental restoration program to characterize, remediate, and close non-Nevada Test Site locations that were used for nuclear testing. Evaluation of radionuclide transport by groundwater from these sites is an important part of the preliminary site risk analysis. These evaluations are undertaken to allow prioritization of the test areas in terms of risk, provide a quantitative basis for discussions with regulators and the public about future work at the sites, and provide a framework for assessing data needs to be filled by site characterization. The Gnome site in southeastern New Mexico was the location of an underground detonation of a 3.5-kiloton nuclear device in 1961, and a hydrologic tracer test using radionuclides in 1963. The tracer test involved the injection of tritium,  $^{90}\text{Sr}$ , and  $^{137}\text{Cs}$  directly into the Culebra Dolomite, a nine to ten-meter-thick aquifer located approximately 150 m below land surface. The Gnome nuclear test was carried out in the Salado Formation, a thick salt deposit located 200 m below the Culebra. Because salt behaves plastically, the cavity created by the explosion is expected to close, and although there is no evidence that migration has actually occurred, it is assumed that radionuclides from the cavity are released into the overlying Culebra Dolomite during this closure process. Transport calculations were performed using the solute flux method, with input based on the limited data available for the site. Model results suggest that radionuclides may be present in concentrations exceeding drinking water regulations outside the drilling exclusion boundary established by DOE. Calculated mean tritium concentrations peak at values exceeding the U.S. Environmental Protection Agency drinking water standard of 20,000 pCi/L at distances of up to almost eight kilometers west of the nuclear test. The transport calculations are most sensitive to changes in the mean groundwater velocity and to variation in assumed sorption properties for sorbing radionuclides, followed by sensitivity to the correlation scale of hydraulic conductivity, the transverse hydrodynamic dispersion coefficient, and the variance in hydraulic conductivity. This modeling was performed to investigate how the uncertainty in various physical parameters affects radionuclide transport at the Gnome site, and to serve as a starting point for discussion regarding further investigation at the site; it was not intended to be a definitive simulation of migration pathways or radionuclide concentration values. Given the sparse data, the modeling results may differ significantly from reality. Confidence in transport predictions can be increased by obtaining more site data, including determining whether the hypothesized release of radionuclides from the cavity to the Culebra Dolomite has occurred, determining an accurate groundwater velocity in the Culebra, and defining sorption properties for possible contaminants.

## CONTENTS

ABSTRACT .....	iii
FIGURES .....	iii
TABLES .....	iv
INTRODUCTION .....	1
METHODOLOGY .....	3
HYDROGEOLOGIC SETTING .....	4
RELEASE SCENARIOS .....	6
DATA .....	9
Source Terms .....	10
Attenuation Factors .....	13
Discharge Mixing Areas .....	14
Distance to Control Plane .....	15
Correlation Scale .....	15
Effective Porosity .....	16
Mean Groundwater Velocity .....	16
Spatial Variability in Hydraulic Conductivity .....	17
RESULTS .....	18
Sensitivity Analyses .....	24
DISCUSSION .....	30
CONCLUSIONS .....	33
REFERENCES .....	34

## FIGURES

1. Setting of the Gnome site in the northern Delaware Basin .....	2
2. Cross section through Project Gnome site showing relation of nuclear cavity, drift, and shaft to local stratigraphy. ....	5
3. Map of the Gnome site showing Gnome and Coach drifts and significant wells. ....	7
4. Timeline of events at the Gnome site. ....	8
5. Detail of T23S, R30E, Section 34 showing hypothesized migration paths to the drilling exclusion boundary. ....	19
6. Modeled tritium concentrations at the drilling exclusion boundary resulting from the Gnome shot and tracer test. ....	19
7. (a) Modeled concentration of $^{36}\text{Cl}$ from the nuclear shot at the drilling exclusion boundary; and (b) Modeled concentration of $^{99}\text{Tc}$ from the nuclear shot at the drilling exclusion boundary. ....	20
8. (a) Modeled concentration of $^{137}\text{Cs}$ from the nuclear shot and tracer test at the drilling exclusion boundary; and (b) Modeled concentration of $^{90}\text{Sr}$ from the nuclear shot and tracer test at the drilling exclusion boundary. ....	22
9. Modeled $^3\text{H}$ , $^{90}\text{Sr}$ , and $^{137}\text{Cs}$ concentrations at the drilling exclusion boundary resulting from the tracer test only. ....	25
10. Modeled peak mean tritium concentrations versus distance west of surface ground zero. ....	25
11. Sensitivity of mean tritium concentration 8 km west of surface ground zero to changes in mean velocity. ....	26
12. Sensitivity of mean tritium concentration 8 km west of surface ground zero to changes in correlation scale. ....	26
13. Sensitivity of mean tritium concentration 8 km west of surface ground zero to changes in variance. ....	28
14. Sensitivity of mean tritium concentration 8 km west of surface ground zero to changes in the hydrodynamic dispersion coefficient. ....	28
15. Sensitivity of modeled $^{90}\text{Sr}$ concentrations crossing the Gnome site boundary to the mean $K_d$ . ....	29
16. Sensitivity of modeled $^{137}\text{Cs}$ concentrations crossing the Gnome site boundary to the mean $K_d$ . ....	29

## TABLES

1. Radionuclides Injected into the Culebra Dolomite in February, 1963 for a Tracer Test Conducted by the U.S. Geological Survey. ....	10
2. Long-lived Radionuclides Produced by the Gnome Nuclear Test .....	11
3. Sorption Coefficients Published For Radionuclides in Contact with the Culebra Dolomite. ....	14
4. Results of Groundwater Transport Calculations for Nuclides with Sorption Information. ....	21
5. Results of Groundwater Transport Calculations for Nuclides without Sorption Information. ....	23

## INTRODUCTION

The U.S. Department of Energy (DOE) and its predecessor agencies are responsible for nuclear weapons research and development as part of the national defense program. These activities include underground nuclear testing, and a small number of such tests have been conducted at sites distant from the Nevada Test Site. The Gnome site is located in southeastern New Mexico, approximately 40 km east-southeast of Carlsbad (Figure 1). The Gnome event was designed primarily to determine the effects resulting from an underground nuclear detonation in salt. The device had a yield of approximately 3.5 KT, and was detonated 360 m below ground surface on December 10, 1961. In addition to the shot, a tracer test performed in 1963 to determine aquifer properties at the site introduced radionuclides to the subsurface environment.

A second nuclear test, known as Project Coach, was planned for the site. Preparations were made for the Coach shot, including the construction of drifts from the Gnome access shaft to the planned ground zero, but the test was never carried out.

DOE has implemented an environmental restoration program with the goal of characterizing, remediating, and closing the offsite nuclear test areas. An early step in this process is performing a preliminary risk analysis of the hazard posed by each site. These analyses will allow prioritization of the sites in terms of risk, provide a quantitative basis for discussions with regulators and the public about future work at the sites, and provide a framework for assessing data needs to be filled by site characterization. Desert Research Institute (DRI) is tasked with performing hydrologic risk evaluations for the groundwater transport pathway. This report details the results of the groundwater-transport evaluation for the Gnome Site in terms of radionuclide concentrations that could cross the site boundary. There are also predictions of distances past which radionuclide concentrations are expected to be below concentrations of regulatory concern. These results will be included with evaluations of risk due to surface sources at Gnome performed by International Technology Corporation to present a comprehensive site risk analysis in a separate report.

The basic scenario evaluated for this assessment is the groundwater transport of radionuclides introduced into the subsurface by the Gnome nuclear shot and tracer test. This assessment strives to be as accurate as possible, but the lack of data requires that significant assumptions be made about release scenarios and several critical transport parameters. As a consequence of these limitations, the results of this modeling are meant to serve merely as a tool to guide further discussion and investigations, not as a definitive assessment of radionuclide migration at the Gnome site. The analysis relies solely on unclassified data available to the general public. Although this may increase the uncertainty of the source term data, and result in the lack of transport calculations for certain radionuclides present at the Gnome site, these issues can be investigated more thoroughly, and with much greater accuracy, after the acquisition of further data regarding contaminant transport at the site. Measured values were used for parameters whenever possible, but given the lack of data, calculations were performed for ranges of certain parameters. The assessment can be made more realistic with the acquisition of additional site data.



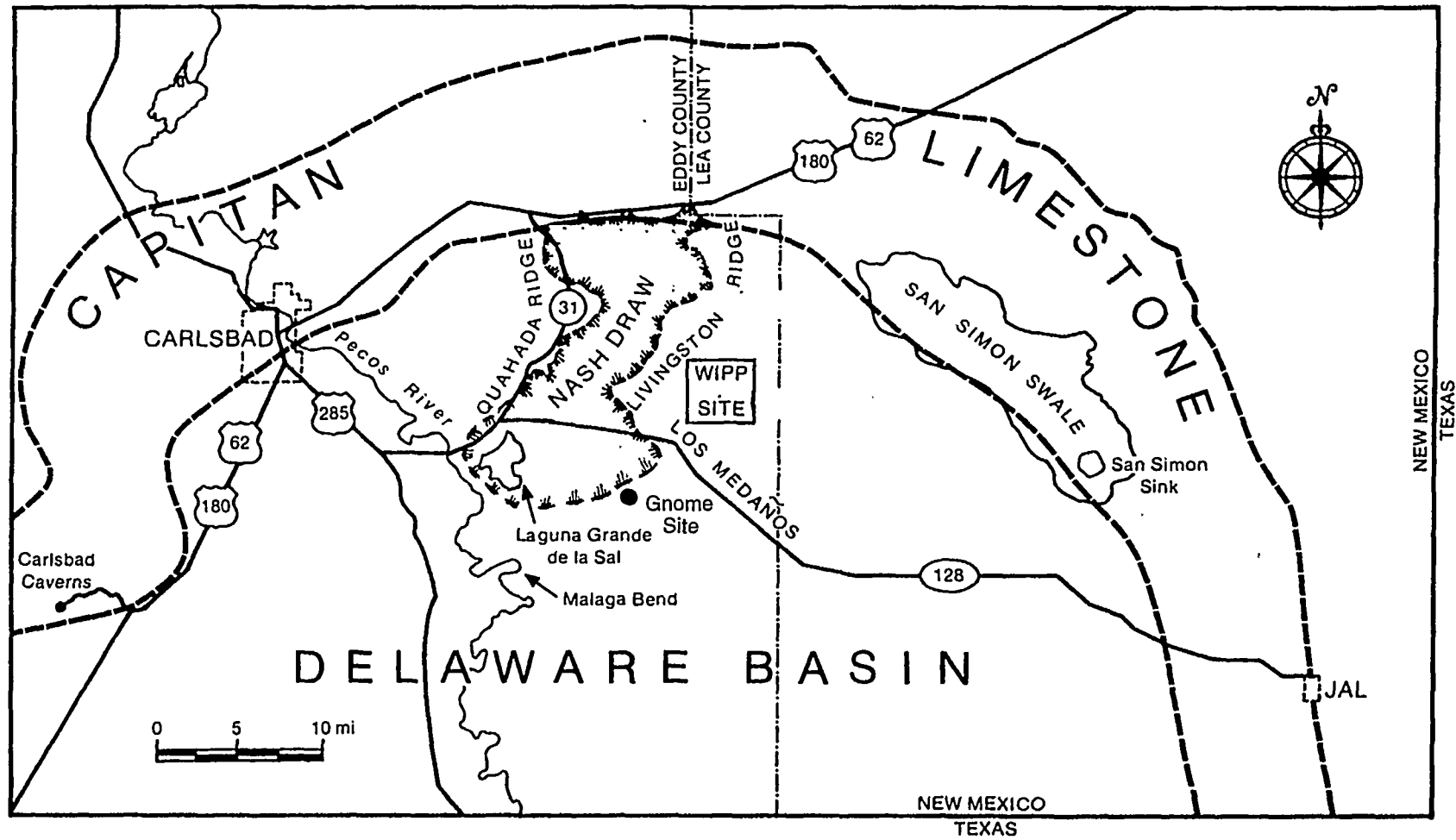


Figure 1. Setting of the Gnome site in the northern Delaware Basin (modified from Lappin, 1988, p. 2).

## METHODOLOGY

A screening tool approach outlined in Daniels *et al.* (1993), Andricevic *et al.* (1994), and Andricevic and Cvetkovic (1996) was used to model radionuclide transport from the Gnome site. The employed modeling approach incorporates real physical phenomena, such as instantaneous and/or slow release from the source, advection, dispersion, sorption, mass transfer, and possible uncertainty in the model parameters. The output is the expected concentration profile as a function of time (e.g., concentration breakthrough curves) at the compliance point downgradient from the source, as well as the uncertainty around the expected concentration resulting from the natural hydrogeologic heterogeneity in general and from the spatially variable groundwater velocity in particular.

The solute flux method is described in detail by Andricevic and Cvetkovic (1996), while important elements of the approach can also be found in Daniels *et al.* (1993) and Andricevic *et al.* (1994). The following summary is derived from these sources, but the reader is directed to these references for a detailed treatment of the method.

The contaminant migration process is described in the solute flux method through the Lagrangian concept of motion following a particle on the Darcy scale. In the absence of direct information on groundwater velocities near Gnome, the mean velocity,  $\bar{U}$ , is calculated using Darcy's law:

$$\bar{U} = \frac{\bar{K} \bar{J}}{\bar{n}_e} \quad (1)$$

where  $\bar{K}$  is the mean hydraulic conductivity,  $\bar{J}$  is the mean hydraulic gradient, and  $\bar{n}_e$  is the mean effective porosity. Hydrogeologic parameters such as  $K$  and  $n_e$  can be highly variable as a result of geologic heterogeneity. Numerous studies of the variability of hydraulic conductivity have concluded that conductivity is generally log-normally distributed (Freeze and Cherry, 1979; Hoeksema and Kitanidis, 1985). Thus, the natural logarithms of hydraulic conductivity data can be described by a normal distribution with a mean  $\mu_{\ln K}$  and variance  $\sigma_{\ln K}^2$ . The variance represents the variability of  $K$  about its mean, and may range from near zero for homogeneous deposits to five, or higher, for extremely variable porous media (Hoeksema and Kitanidis, 1985). Because it is distributed in space,  $K$  usually has some degree of spatial correlation. The negative exponential function is often used to describe the  $K$  correlation structure because it is found to correspond to log  $K$  data and is easy to use. The correlation length of  $K$ ,  $\lambda$ , represents the distance beyond which data points show weak correlation. The higher the value of  $\lambda$ , the greater the spatial continuity of  $K$ . When the log-normal distribution and the negative exponential covariance function are assumed, the heterogeneous, isotropic hydraulic conductivity field can be statistically characterized by three parameters:  $\mu_{\ln K}$ ,  $\sigma_{\ln K}^2$ , and  $\lambda$ .

If the parameters on the right-hand side of the Darcy equation are log-normally distributed, then so is  $\bar{U}$  and the estimate of the mean velocity is  $\mu_{\ln U} = \mu_{\ln K} + \mu_{\ln J} - \mu_{\ln n_e}$ . The variance of the estimated mean  $U$ ,  $\sigma_{\ln U}^2$ , can be calculated as the sum of the variances of the other parameters, if

sufficient data are available. The estimation error in  $U$ ,  $\sigma_{\ln U}^2$ , represents the magnitude of uncertainty in the estimate of  $U$  contributed by the estimation errors of  $K$ ,  $J$ , and  $n_e$ . The magnitude of the uncertainty in the mean velocity,  $\sigma_{\ln U}^2$ , depends on the number of measurements used to estimate the parameters in the Darcy equation. In the case of independent measurements,  $\sigma_{\ln U}^2 = \sigma_{\ln U}^2/N$ , where  $\sigma_{\ln U}^2$  is the variance in the velocity field and  $N$  is the number of measurements. For spatially correlated measurements,  $\sigma_{\ln U}^2$  is scaled by  $N^{-1}[1+\bar{\rho}(N-1)]$ , where  $\bar{\rho}$  is an averaged spatial correlation between data points.

The solute flux method evaluates movement of a solute from the source to a plane perpendicular to the direction of flow. Aquifer heterogeneity is included and represented by the variance of log-hydraulic conductivity,  $\sigma_{\ln K}^2$ , and the hydraulic conductivity integral scale,  $\lambda$ . The combination of the spatial variability of aquifer properties and the uncertainty in the estimates of these properties causes the solute flux to be a random function described by a probability density function (PDF). The mean and variance of the solute flux are converted to the flux-averaged concentration needed for risk calculations by dividing by the groundwater flux,  $Q$ . The first two moments of the flux-averaged concentration are important in determining the total risk level. The larger the magnitude of variance in the flux-averaged concentrations, the larger the maximum potential risk.

## HYDROGEOLOGIC SETTING

The geology and hydrogeology of the Gnome site are described by Gard (1968), Cooper (1962a), Cooper (1962b), and Cooper and Glanzman (1971); data regarding the Culebra Dolomite from investigations at the Waste Isolation Pilot Plant (WIPP) site, located approximately 10 km northeast of the Gnome site (Figure 1), are provided by Cauffman *et al.* (1990), Lowenstein (1987), and Snyder (1985); and Pohlmann and Andricevic (1994) model the migration of tritium introduced into the Culebra by the tracer test.

The Gnome event was conducted at a depth of 360 m below ground surface, within the Salado Formation (Figure 2), a Permian salt deposit composed primarily of halite and polyhalite. The Salado is approximately 500 m thick at the site, but the halite is not vertically continuous, as thin sandstone and anhydrite members are present (Gardner and Sigalove, 1970; Gard, 1968).

The only aquifer present at the site is the Culebra Dolomite Member of the Rustler Formation (Cooper and Glanzman, 1971). Cooper (1962a) describes the Culebra as a "grayish-white" dolomite in which fractures are the primary means by which water is stored and transported. It is approximately 9.1 m thick at the Gnome site, and its bottom is about 204 m above the shot point (Cooper and Glanzman, 1971).

Most groundwater in the Gnome area is too saline for human consumption, but it is used by livestock (Cooper and Glanzman, 1971). Chloride and sulfate concentrations as high as 10,600 and 3,047 mg/L, respectively, have been reported, and most water samples contain concentrations of iron and magnesium in excess of drinking water standards (Cooper, 1962a).

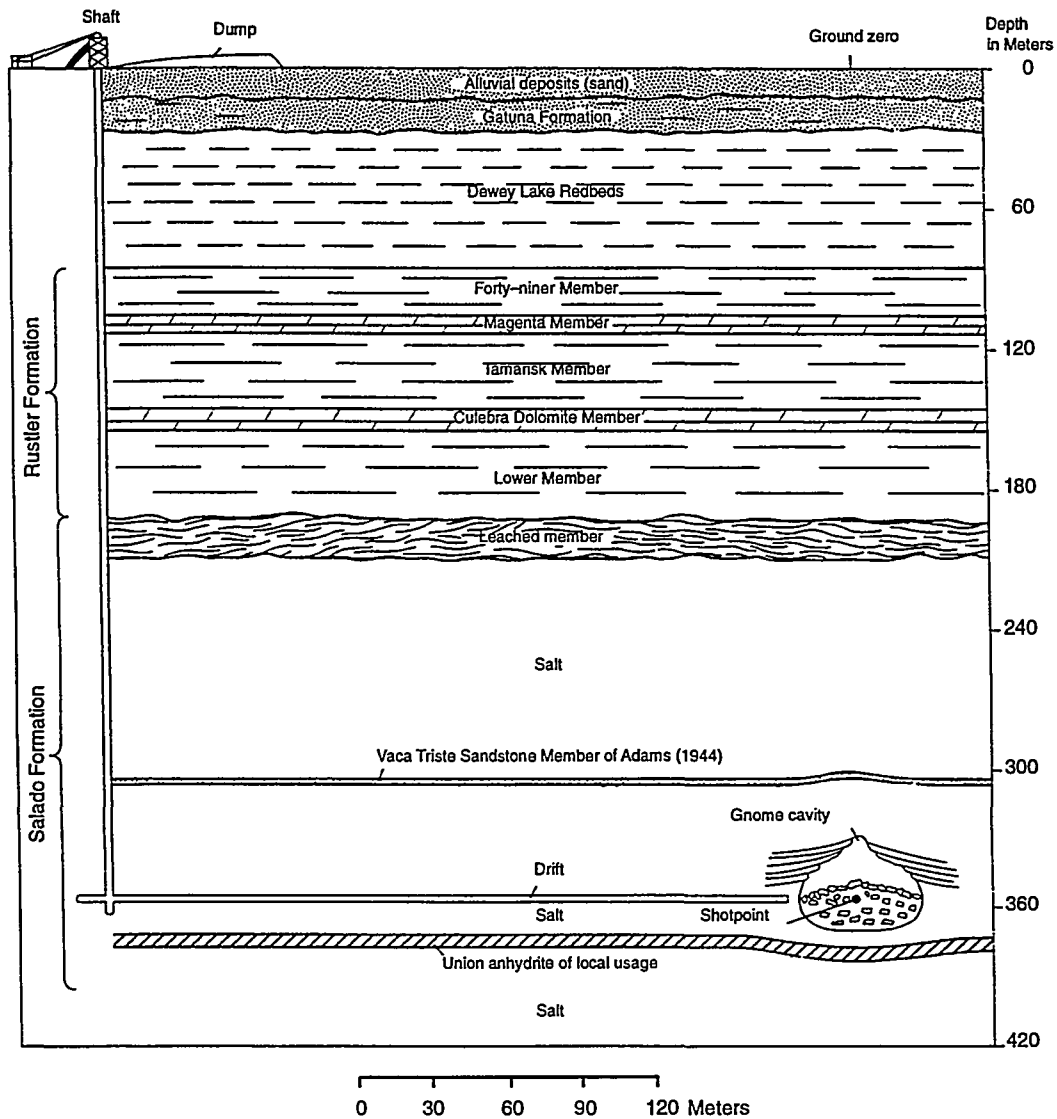


Figure 2. Cross section through Project Gnome site showing relation of nuclear cavity, drift, and shaft to local stratigraphy (after Gard, 1968).

The recharge area for the Culebra is not clearly defined. Some recharge occurs in areas where the Culebra is exposed as an outcrop (Cooper, 1962a), and other recharge takes place via sinkholes in the Nash Draw collapse feature (Figure 1) (Cooper, 1962b). Overlying Triassic sandstone may also provide some water, but the regional flow pattern suggests a primary recharge area to the north and east (Cooper, 1962b). Although some interconnection with the overlying rock has been hypothesized, it is not directly supported by any known evidence. Groundwater flows in a westward or southwestward direction from the site (Cooper, 1962a; Cooper and Glanzman, 1971). It is thought that the Pecos River is the primary discharge area for the Culebra (Cooper, 1962a), particularly in an area of springs at Malaga Bend. Pohlmann and Andricevic (1994) note that transmissivity in the Culebra increases from east to west in the Gnome area. This is due to increased fracturing of the

dolomite as the result of greater dissolution of underlying halite, and increased thickness of the Culebra.

Pohlmann and Andricevic (1994) used analytic solutions to investigate potential migration of tritium introduced by the tracer test. Their results suggest that significant spreading of tritium will occur in the Culebra, causing a very small amount of mass to reach the Pecos River (10 to 15 km from the Gnome site) within the time elapsed since the tracer test. It is predicted that tritium concentrations are reduced by dilution and dispersion during transport. About 95% of the mass remaining after decay is predicted to have remained within 1 km downgradient.

## RELEASE SCENARIOS

There are four potential sources for groundwater contamination by radionuclides at the Gnome site. Two of these are near-surface sources: fallout from venting of the shot and surface contamination from site activities (*e.g.*, drillback operations). The other two sources are in the subsurface: radioactive material in the shot cavity and drifts, and radioactive tracers injected into the Culebra Dolomite through well USGS-8 (Figure 3).

The potential impact of the near-surface sources on water quality is minor compared to the possible impact of the subsurface sources. Surface venting from the Gnome shaft and ventilation lines, consisting of steam and gray smoke, began to occur seven minutes after the nuclear detonation, and continued through the following day. The radioactive elements that vented were volatile and noble gases such as  $^{131}\text{I}$ ,  $^{133}\text{Xe}$ ,  $^{85}\text{Kr}$ , and  $^{37}\text{Ar}$ , as well as  $^3\text{H}$  in the steam. The fallout was carried in a northwesterly direction from the shaft, and that section of the site had slightly elevated radiation levels as of 1978 (Reynolds Electrical & Engineering Co., Inc., 1978). Surface contamination was reduced during two decontamination projects that led to unrestricted use of the land surface (Reynolds Electrical & Engineering Co., Inc., 1981). Radionuclides on the land surface would have to travel over 150 m through the unsaturated zone to reach the Culebra Dolomite. Given the semi-arid climate and sorptive properties of decay products such as  $^{137}\text{Cs}$ , such transport is expected to be very slow, if it occurs at all. Because the surface sources are considered separately in terms of characterization and remediation, only the two subsurface sources are analyzed in this report.

The tracer test at the Gnome site was performed in February and March, 1963. To calculate a dilution factor for the aquifer, unknown quantities of tritium and fluorescein were injected into the Culebra prior to the tracer test (Beetem and Angelo, 1964). The tracer test involved the injection of radionuclides into well USGS-8, with well USGS-4 acting as a pumping well from which water was piped back to USGS-8 for reinjection (Grove and Beetem, 1971). No records exist of any attempt to remove the radionuclides injected into the Culebra. As a result, the release scenario for the tracer test involves the simple instantaneous release of a slug of radionuclides through USGS-8 into the aquifer.

The release scenario for the shot is much more hypothetical than that for the tracer test, as no direct evidence exists that the migration of radionuclides from the cavity to the Culebra has occurred. Salt is typically highly impermeable, and thus not a likely transport path for groundwater, but it

behaves plastically, meaning that the cavity created by the blast cannot be expected to remain open indefinitely. If any pathway to the Culebra were present during the closure of the cavity, water from the cavity could be squeezed out along this pathway, due to the “collapsing” salt. Because the possibility of migration resulting from cavity closure does exist, a scenario for this type of release was postulated, and used to generate a conservative estimate of radionuclide migration from the Gnome site.

Based on data (Munson *et al.*, 1989) from the WIPP site, it was estimated that closure of the Gnome cavity in its original state to the point that water would actually be squeezed from the cavity would have taken from 25 to 51 years after the shot. However, during a surface cleanup operation in 1979 (18 years after the nuclear test), the Gnome cavity was “filled to near capacity” with contaminated materials (Reynolds Electrical and Engineering Co., Inc., 1981), meaning that minimal void space remained, and thus any cavity closure subsequent to that point could result in water being squeezed immediately from the cavity. In cavities which have high pore pressure from internal gases, the closure process will generally be slowed (Butcher, B., Sandia National

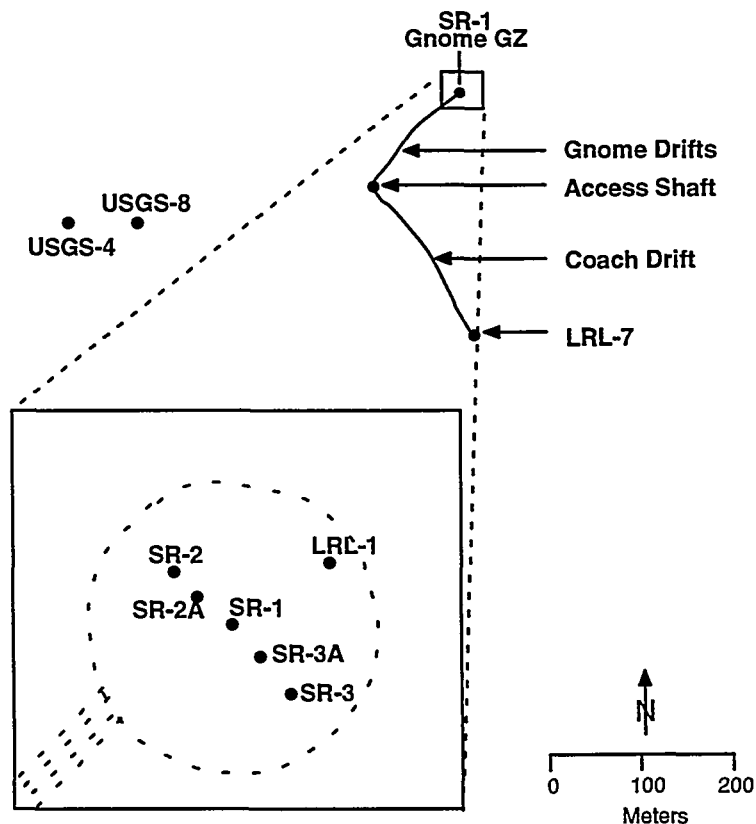


Figure 3. Map of the Gnome site showing Gnome and Coach drifts and significant wells. Detail map shows the Gnome cavity area, and includes hypothesized well locations for SR-2 and SR-3 based on available descriptions. Well DD-1 is another cavity re-entry well, but no details exist regarding its exact location in the area above the cavity.

Laboratories, personal communication, 1996), but postshot venting of gases, as described by DOE (1982) precludes this being a mitigating factor at the Gnome site. Given the modified cavity condition, it was estimated that once the cavity was filled completely in 1979, water began to be squeezed out due to cavity closure. It was estimated that it would take 12 years for the natural closure process to eject all the water from the cavity. Thus, leakage of contaminants from the cavity is postulated to occur between 1979 and 1991 (Figure 4).

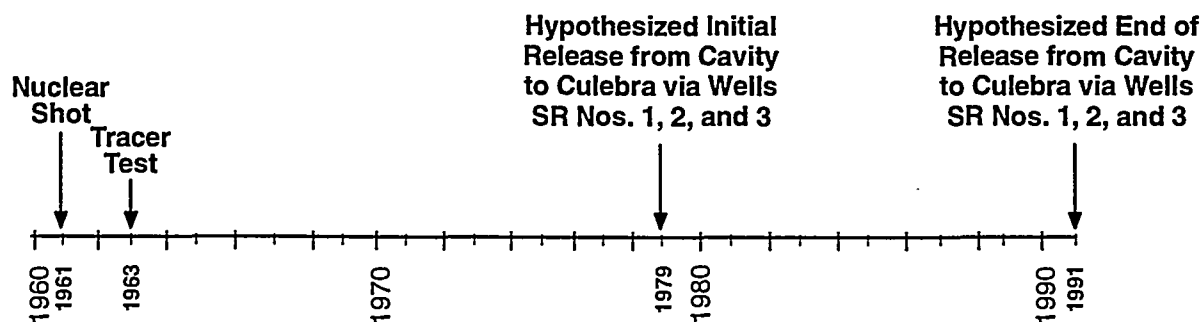


Figure 4. Timeline of events at the Gnome site.

The Gnome cavity was connected to the surface by the access shaft and drifts, and by at least seven wells drilled for re-entry activities. Four of the re-entry wells (LRL-2A, LRL-3A (also referred to as SR-2A and SR-3A), LRL-7, and DD-1) were constructed after the shot, and all but LRL-7 and DD-1 were plugged during the 1979 decontamination operation (Reynolds Electrical and Engineering Co., Inc., 1981). Because these wells were never subjected to the effects of the shot, if properly constructed and sealed, there should be no risk of them acting as conduits for water from the cavity to the Culebra. The Gnome shaft was “rehabilitated” (no details of this process are available) as part of Project Coach (Department of Energy, 1982), so it is also not likely to serve as a conduit to the Culebra. Three re-entry wells (SR No. 1, SR No. 2 and SR No. 3) were drilled and filled with “weak grout” prior to the shot (Hale *et al.*, 1961). The blast effects were evident at the surface, forming a dome 0.52 m high at surface ground zero (SGZ), and 0.08 m high from 61 to 122 m away (Hale *et al.*, 1961). As a result, the casing of hole SR No. 1 was “sheared at ground surface where a concrete slab surrounded it,” and the hole was open to a depth of 145 m; the casing of SR No. 2 was parted and displaced at several depths, including 53, 92, and 182 m. Attempts to redrill SR No. 2 failed due to the damage. Although no description of damage to SR No. 3 is given, it is noted that redrilling attempts “met with results similar to SR No. 2,” suggesting at least a similar amount of damage to the casing (Hale *et al.*, 1961).

Although it is possible that these three wells were resealed after the shot and subsequent attempts at re-entry, no mention of this is made in any available literature. As a result, it was assumed that these wells were left unsealed, and that the damage caused by the shot could allow them to act

as conduits for flow from the cavity to the Culebra. Wells SR No. 2 and SR No. 3 were located approximately 9.1 m on either side of SR No. 1, which was located at SGZ (Hale *et al.*, 1961). Since the shot produced a dome at ground surface, it is reasonable to assume that fracturing occurred in the Culebra, and that any water squeezed from the cavity up the re-entry holes would flow fairly rapidly through the entire fractured area between them. It was thus assumed that the water from the Gnome cavity was introduced into the Culebra throughout this area over a 12-year period (the most conservative value estimated for the time it would take for salt "collapse" to squeeze all water from the cavity into the Culebra), beginning in 1979.

The major events modeled for this study are the nuclear shot in 1961, the tracer test in 1963, and the release of radionuclides from the Gnome cavity into the Culebra via wells SR Nos. 1, 2, and 3. This release process, as modeled, begins in 1979 (18 years after the shot), and takes place over a 12-year period (1979 to 1991).

It is important to note that wells SR Nos. 1, 2, and 3 may have been sealed, in which case radionuclides from the shot would have very little likelihood of migrating away from the cavity through the Culebra. In addition, the cavity closure rate estimate is quite rudimentary, so even if water from the cavity were to flow into the Culebra, the actual time of release may be different than the 12 years used in this study.

## DATA

The specific conceptual model evaluated in this exposure assessment is that of groundwater flow transporting radionuclides from the Gnome shot and tracer test through the Culebra Dolomite to hypothetical receptor locations downgradient. By virtue of describing the solute flux through the Lagrangian concept of motion (following a particle on the Darcy scale), the analytical solution is actually independent of the transport medium, relying simply on the assigned transport properties. The only assumption required is that the particle trajectory not deviate significantly from the mean flow direction. This assumption is imbedded in the first-order approximation used to derive the arrival time moments of the moving plume (see Dagan *et al.*, 1992).

The method allows for matrix diffusion, a potentially important process by which solutes are removed from high velocity fracture flowpaths into adjoining matrix blocks. Within the matrix, where velocities are much lower than those in fractures, radioactive decay acts as an effective natural remediating process. Due to the lack of data regarding matrix diffusion at the Gnome site, the process was not considered for this report. Because matrix diffusion can significantly reduce radionuclide concentrations, neglecting it will result in conservative model output values.

The parameters used for the transport calculations are discussed in detail below. In some cases, lack of data requires that significant assumptions be made regarding the appropriate input values. Parametric uncertainty in all of the hydraulic properties can be included through uncertainty in the estimate of the mean velocity, but because data were estimated, sensitivity analyses were performed on parameter ranges instead.



## Source Terms

The source term used for the tracer test is equal to the amount of injected radionuclides, as described in Table 1. Pre-test injection of tritium, which was not quantified, was assumed to be minimal, and thus not included in the source term for the test. The amount of tritium injected during the tracer test is not reported consistently throughout the available literature. Although some sources, such as Gardner and Sigalove (1970), report that 50 Ci were injected into USGS-8, this appears to be a misconception based on the fact that the purchase of up to 50 Ci of  $^3\text{H}$  was authorized for the test (Beetem and Angelo, 1964), and this figure is frequently mentioned in planning documents. Tritium injection is also frequently described as being 20 Ci, but this appears to be derived from rounding up the actual figure of 18.5. In discussing the results of the test, Grove and Beetem (1971) describe a total tritium injection of approximately 18.5 Ci.

TABLE 1. RADIONUCLIDES INJECTED INTO THE CULEBRA DOLOMITE IN FEBRUARY, 1963 DURING A TRACER TEST CONDUCTED BY THE U.S. GEOLOGICAL SURVEY.

Isotope	Activity Injected, pCi
$^3\text{H}$	$1.85 \times 10^{13}$
$^{137}\text{Cs}$	$1.0 \times 10^{13}$
$^{131}\text{I}$	$4.0 \times 10^{12}$
$^{90}\text{Sr}$	$1.0 \times 10^{13}$

The contaminant mass in the cavity, drifts, and shaft is more difficult to quantify. The main components of this source are radionuclides placed in the zero room for the isotope production study, and the Gnome nuclear test itself. The radionuclides in the post-shot environment are from four primary sources: radioisotopes placed in or near the device as part of an isotope production study, radioisotopes produced by neutron activation, radionuclides produced by the fission of  $^{239}\text{Pu}$ , and any of the nuclear fuel from the device that was not consumed by the test. Some information about the Gnome test remains classified. For example, the list of the types and amounts of isotopes added to the device for the production study is classified, though it is known that the most significant isotope was tritium (Gardner and Sigalove, 1970). Although no information is given for other radionuclides, Nathans (1965) reports that 0.06 g of tritium were placed in the zero room, equivalent to about  $6.0 \times 10^{14}$  pCi. The amount (if any) of unburned nuclear fuel (including isotopes of Pu, U, and H) remains classified as well. Given the purpose of this modeling as a planning tool, and the importance of public access to achieving that purpose, no classified data are included in the analysis. This results in an underestimation of nuclides included in the unburned nuclear fuel, and an uncertainty in the activation and fission products that can be reduced in future transport calculations. Gardner and Sigalove (1970) calculate the neutron activation products and fission products that resulted from the Gnome test (Table 2), and these unclassified values, along with the unclassified value for  $^3\text{H}$  added for the isotope production study, are used to represent the primary source term in the cavity.

Post-shot surface venting caused an unknown amount of tritium and other radioactive gases to be released to the atmosphere. The radionuclide source term for the cavity has not been reduced

to account for the venting, because the mass that escaped is unknown. Contaminated soil, muck, and materials (such as pipes and tanks) were disposed of by placing or slurring them into the underground workings at Gnome. No detailed radionuclide inventory of this material has been found, but as it presumably originated from the Gnome shot, it is most likely accounted for in Table 2. In the case of tritium, the  $6.0 \times 10^{14}$  pCi placed in the zero room (Nathans, 1965) was added to the  $1.1 \times 10^{14}$  pCi reported by Gardner and Sigalove (1970) to obtain the value given in Table 2. Since the release scenario for the nuclear test includes a delay of 18 years after the shot, the radionuclide masses calculated by Gardner and Sigalove (1970) were reduced to account for the decay that occurred prior to the start of migration (Table 2).

The amount of each radionuclide source term available for transport in groundwater is called the "hydrologic source term." The hydrologic source term is often smaller than the total radiologic source term because many radionuclides cannot be transported by groundwater, due to incorporation in the relatively insoluble melt glass or rapid decay rates (Smith *et al.*, 1995). For example, most postshot surveys conducted by re-entering the Gnome cavity after the shot found the majority of the radionuclides confined to melt (or glass) zones at the base of the cavity (Rawson *et al.*, 1965). Studies of this material revealed that almost all of the fission products remained with the salt impurities when samples were dissolved in water or remelted to separate the NaCl (Rawson *et al.*, 1965, Nathans, 1965). Those nuclides that do leach slowly out of melt debris often have strong sorbing properties that also limit migration. Generally, tritium is considered to be of the greatest concern for radionuclide transport for the first 100 to 200 years after a test, because it is present in large concentration, and is very mobile in water (Smith *et al.*, 1995).

TABLE 2: LONG-LIVED RADIONUCLIDES PRODUCED BY THE GNOME NUCLEAR TEST (from Gardner and Sigalove, 1970). The mass at 18 years after the Gnome event was used as the beginning concentration for transport from the nuclear test to coincide with the start of radionuclide release to the Culebra resulting from cavity closure (see text).

Nuclide	Source*	Half-life (yr)	Initial Activity (pCi)	Activity 18 yrs after shot (pCi)	Activity in 1996 (pCi)
$^3\text{H}$	a,p,t	$1.23 \times 10^1$	$7.10 \times 10^{14}$	$2.58 \times 10^{14}$	$9.88 \times 10^{13}$
$^{14}\text{C}$	a	$5.73 \times 10^3$	$4.90 \times 10^7$	$4.89 \times 10^7$	$4.88 \times 10^7$
$^{22}\text{Na}$	a	$2.61 \times 10^0$	$1.70 \times 10^9$	$1.42 \times 10^7$	$1.54 \times 10^5$
$^{36}\text{Cl}$	a	$3.01 \times 10^5$	$5.60 \times 10^{11}$	$5.60 \times 10^{11}$	$5.60 \times 10^{11}$
$^{39}\text{Ar}$	a	$2.69 \times 10^2$	$9.10 \times 10^{11}$	$8.69 \times 10^{11}$	$8.32 \times 10^{11}$
$^{40}\text{K}$	a	$1.30 \times 10^9$	$3.85 \times 10^5$	$3.85 \times 10^5$	$3.85 \times 10^5$
$^{41}\text{Ca}$	a	$1.03 \times 10^5$	$8.40 \times 10^8$	$8.40 \times 10^8$	$8.40 \times 10^8$
$^{45}\text{Ca}$	a	$4.50 \times 10^{-1}$	$1.29 \times 10^{13}$	$1.18 \times 10^1$	$5.04 \times 10^{-11}$
$^{54}\text{Mn}$	a	$8.60 \times 10^{-1}$	$5.95 \times 10^7$	$2.99 \times 10^1$	$3.36 \times 10^5$
$^{55}\text{Fe}$	a	$2.70 \times 10^0$	$1.72 \times 10^{10}$	$1.69 \times 10^8$	$2.16 \times 10^6$
$^{57}\text{Co}$	a	$7.00 \times 10^{-1}$	$7.00 \times 10^6$	$1.28 \times 10^{-1}$	$6.26 \times 10^9$
$^{60}\text{Co}$	a	$5.27 \times 10^0$	$2.03 \times 10^8$	$1.90 \times 10^7$	$2.04 \times 10^6$

TABLE 2: LONG-LIVED RADIONUCLIDES PRODUCED BY THE GNOME NUCLEAR TEST  
(Continued).

Nuclide	Source*	Half-life (yr)	Initial Activity (pCi)	Activity 18 yrs after shot (pCi)	Activity in 1996 (pCi)
<sup>63</sup> Ni	a	1.00 x 10 <sup>2</sup>	5.60 x 10 <sup>7</sup>	4.94 x 10 <sup>7</sup>	4.39 x 10 <sup>7</sup>
<sup>65</sup> Zn	a	6.60 x 10 <sup>-1</sup>	3.01 x 10 <sup>9</sup>	1.86 x 10 <sup>1</sup>	3.30 x 10 <sup>-7</sup>
<sup>85</sup> Kr	a,f	1.07 x 10 <sup>1</sup>	4.50 x 10 <sup>13</sup>	1.40 x 10 <sup>13</sup>	4.66 x 10 <sup>12</sup>
<sup>87</sup> Rb	f	4.90 x 10 <sup>10</sup>	7.35 x 10 <sup>4</sup>	7.35 x 10 <sup>4</sup>	7.35 x 10 <sup>4</sup>
<sup>90</sup> Sr	f,t	2.91 x 10 <sup>1</sup>	2.40 x 10 <sup>14</sup>	1.56 x 10 <sup>14</sup>	1.04 x 10 <sup>14</sup>
<sup>94</sup> Nb	f	2.40 x 10 <sup>4</sup>	7.00 x 10 <sup>6</sup>	7.00 x 10 <sup>6</sup>	6.99 x 10 <sup>6</sup>
<sup>98</sup> Tc	f	4.20 x 10 <sup>6</sup>	1.61 x 10 <sup>4</sup>	1.61 x 10 <sup>4</sup>	1.61 x 10 <sup>4</sup>
<sup>99</sup> Tc	f	2.13 x 10 <sup>5</sup>	8.75 x 10 <sup>10</sup>	8.75 x 10 <sup>10</sup>	8.75 x 10 <sup>10</sup>
<sup>106</sup> Ru	f	1.02 x 10 <sup>0</sup>	1.40 x 10 <sup>16</sup>	6.84 x 10 <sup>10</sup>	6.59 x 10 <sup>5</sup>
<sup>102</sup> Rh	f	2.90 x 10 <sup>0</sup>	1.01 x 10 <sup>9</sup>	1.37 x 10 <sup>7</sup>	2.35 x 10 <sup>5</sup>
<sup>107</sup> Pd	a	6.50 x 10 <sup>6</sup>	1.28 x 10 <sup>6</sup>	1.28 x 10 <sup>6</sup>	1.28 x 10 <sup>6</sup>
<sup>110m</sup> Ag	a,f	6.80 x 10 <sup>-1</sup>	6.90 x 10 <sup>12</sup>	7.45 x 10 <sup>4</sup>	2.23 x 10 <sup>-3</sup>
<sup>113m</sup> Cd	f	1.41 x 10 <sup>1</sup>	1.19 x 10 <sup>10</sup>	4.91 x 10 <sup>9</sup>	2.13 x 10 <sup>9</sup>
<sup>115</sup> In	f	6.00 x 10 <sup>14</sup>	3.39 x 10 <sup>-1</sup>	3.39 x 10 <sup>-1</sup>	3.39 x 10 <sup>-1</sup>
<sup>125</sup> Sb	f	2.76 x 10 <sup>0</sup>	1.36 x 10 <sup>14</sup>	1.48 x 10 <sup>12</sup>	2.07 x 10 <sup>10</sup>
<sup>129</sup> I	f	1.67 x 10 <sup>7</sup>	5.60 x 10 <sup>8</sup>	5.60 x 10 <sup>8</sup>	5.60 x 10 <sup>8</sup>
<sup>134</sup> Cs	a,f	2.07 x 10 <sup>0</sup>	1.16 x 10 <sup>12</sup>	2.75 x 10 <sup>9</sup>	9.15 x 10 <sup>6</sup>
<sup>135</sup> Cs	a	2.30 x 10 <sup>6</sup>	7.82 x 10 <sup>-2</sup>	7.82 x 10 <sup>-2</sup>	7.82 x 10 <sup>-2</sup>
<sup>137</sup> Cs	f,t	3.02 x 10 <sup>1</sup>	7.00 x 10 <sup>14</sup>	4.63 x 10 <sup>14</sup>	3.13 x 10 <sup>14</sup>
<sup>138</sup> La	a	1.00 x 10 <sup>11</sup>	8.87 x 10 <sup>3</sup>	8.87 x 10 <sup>3</sup>	8.87 x 10 <sup>3</sup>
<sup>144</sup> Nd	f	2.10 x 10 <sup>15</sup>	1.92 x 10 <sup>0</sup>	1.92 x 10 <sup>0</sup>	1.92 x 10 <sup>0</sup>
<sup>147</sup> Pm	f	2.62 x 10 <sup>0</sup>	2.24 x 10 <sup>15</sup>	1.92 x 10 <sup>13</sup>	2.14 x 10 <sup>11</sup>
<sup>147</sup> Sm	f	1.10 x 10 <sup>11</sup>	5.25 x 10 <sup>4</sup>	5.25 x 10 <sup>4</sup>	5.25 x 10 <sup>4</sup>
<sup>151</sup> Sm	a,f	9.00 x 10 <sup>1</sup>	3.10 x 10 <sup>13</sup>	2.69 x 10 <sup>13</sup>	2.36 x 10 <sup>13</sup>
<sup>152</sup> Eu	a	1.35 x 10 <sup>1</sup>	3.90 x 10 <sup>13</sup>	1.55 x 10 <sup>13</sup>	6.45 x 10 <sup>12</sup>
<sup>154</sup> Eu	a,f	8.59 x 10 <sup>0</sup>	9.94 x 10 <sup>12</sup>	2.33 x 10 <sup>12</sup>	5.90 x 10 <sup>11</sup>
<sup>155</sup> Eu	f	4.90 x 10 <sup>0</sup>	4.20 x 10 <sup>14</sup>	3.29 x 10 <sup>13</sup>	2.98 x 10 <sup>12</sup>
<sup>153</sup> Gd	a	6.60 x 10 <sup>-1</sup>	8.98 x 10 <sup>8</sup>	5.56 x 10 <sup>0</sup>	9.84 x 10 <sup>-8</sup>
<sup>158</sup> Tb	a	1.50 x 10 <sup>2</sup>	6.76 x 10 <sup>7</sup>	6.22 x 10 <sup>7</sup>	5.75 x 10 <sup>7</sup>

\*a = Produced by neutron activation in salt.

t = Nuclide also used in the tracer test, though that mass is not included in this table. See Table 1.

f = Produced by neutron-induced fission of <sup>239</sup>Pu.

p = Added to zero room as part of isotope production study.

Non-radioactive materials were also added to the shot for shielding and support. These included several tons each of iron, lead, polyethylene, and wood, and smaller quantities of aluminum

and brass. These materials reacted with the surrounding rock as a result of the nuclear explosion, and formed a wide variety of iron-rich minerals, such as magnetite, olivine, galena, and lead hydrochloride (Nathans, 1965). Neither the transport of non-radioactive species, nor the potential activation of any of the shielding material, are considered in this study.

It should be emphasized that the source term used here is based solely on unclassified data. As a result, the true source could differ from that used for the calculations presented here, due to the combined effects of the post-shot venting, the classified radionuclides emplaced for the isotope production study, and the possible presence of nuclear fuel not consumed by the test.

### Attenuation Factors

As discussed by Smith *et al.* (1995), there are a number of factors that complicate the release function of various radionuclides from an underground test: heterogeneous spatial and chemical distribution (in melt matrix, on surfaces, etc.), solubility, sorption, and colloid formation. Smith *et al.* (1995) emphasize the importance of time in evaluating the transition from radiologic to hydrologic source term because the relative importance of the radionuclides changes during decay. All of these factors are essentially unknown for the Gnome test, though the distribution of nuclides and timing of release can be reasonably estimated for the tracer test.

Distribution coefficients for a number of radionuclides in contact with the Culebra Dolomite have been measured in the laboratory (Janzer *et al.*, 1962; Lynch and Dosch, 1980; a summary of previous work presented in Pearson *et al.*, 1987).  $K_d$  is strongly dependent on mineralogy and the geochemical environment (groundwater ionic composition, Eh, and most importantly, pH), and thus can vary widely *in situ*, as well as in laboratory tests conducted under different conditions. In addition, estimation of sorption behavior based on a  $K_d$  assumes a linear isotherm, or alternatively, evaluation of sorption at a single contaminant concentration. Sorption isotherms for many strongly sorbing radionuclides are highly non-linear. All sorption measurements published for the Culebra Dolomite were performed on crushed samples. Values reported by Janzer *et al.* (1962) are notably higher than those reported by Lynch and Dosch (1980) for Sr and Cs (Table 3). Though Janzer *et al.* (1962) used samples of Culebra Dolomite from the Gnome shaft, while Lynch and Dosch (1980) used cores of the Culebra from drillholes around the WIPP site, the values reported by Lynch and Dosch (1980) are used here because the laboratory methodology appears to be more rigorous, and the values are lower and thus more conservative (allowing greater transport). The values used for Eu are the "apparent" values reported by Lynch and Dosch (1980) that exclude sorption attributed to the experimental apparatus (e.g., container walls), rather than the values as reported by Pearson *et al.* (1987).

The  $K_d$  used for the transport calculations is a spatially variable distribution coefficient made dimensionless by multiplying by the ratio of the bulk density of the Culebra ( $\rho_B$ ) (2.5 g/cm<sup>3</sup> (Dickey and Gard, 1962)) and the effective porosity ( $\theta$ ) (0.10 (Cooper and Glanzman, 1971)). It is assumed to be a stationary random field described by a mean ( $\bar{K}_d$ ) and variance ( $\sigma^2_{K_d}$ ). The variance in  $K_d$  in the flow field was calculated by taking the reported range from Lynch and Dosch (1980), dividing by four, and squaring the result. Although the solute flux method used for transport calculations can

consider correlations between  $K_d$  and hydraulic conductivity (Andricevic and Cvetkovic, 1996), no correlation was assumed in these calculations. Of the radionuclides listed in Table 2, only 12 had sorption data available, and thus transport calculations including sorption estimates could only be performed for these 12 ( $^3\text{H}$ ,  $^{90}\text{Sr}$ ,  $^{137}\text{Cs}$ ,  $^{135}\text{Cs}$ ,  $^{134}\text{Cs}$ ,  $^{36}\text{Cl}$ ,  $^{99}\text{Tc}$ ,  $^{98}\text{Tc}$ ,  $^{129}\text{I}$ ,  $^{155}\text{Eu}$ ,  $^{154}\text{Eu}$ ,  $^{152}\text{Eu}$ ). It should be emphasized that the  $K_d$  values available for these nuclides are uncertain, and that the transport calculations do not include all the other possible attenuation factors described by Smith *et al.* (1995). Transport for the remainder of the source nuclides did not include any retardation factors, and are thus extremely conservative, because many of these nuclides can be expected to have strong sorption properties, or to occur in chemical forms with low solubility.

TABLE 3. SORPTION COEFFICIENTS PUBLISHED FOR RADIONUCLIDES IN CONTACT WITH THE CULEBRA DOLOMITE.

	Janzer <i>et al.</i> (1962)	Pearson <i>et al.</i> (1987) ( $K_d$ , ml/g)	Lynch & Dosch (1980)	$K_d * Q_B / \phi$	$\bar{K}_d$ (dimensionless)	$\sigma^2 K_d$
Sr	9	0.3-0.6	0.3-0.6	7.5-15	11	3.5
Cs	176	9.0-68.3	9.0-68.3	225-1708	967	$1.4 \times 10^5$
Fission Products	861-1570					
Eu		$0.9 \times 10^4$ - $1.2 \times 10^4$	1236-1592	30,900- 39,800	35,350	$5 \times 10^6$
U		1.1-7.4				
Pu		$1.1 \times 10^3$ - $4.5 \times 10^3$	202-877			
Am		$4.8 \times 10^3$ - $7.7 \times 10^3$	228-383			
Tc			0	0	0	0
$^3\text{H}$					0	0
$^{36}\text{Cl}$					0	0
$^{129}\text{I}$					0	0

### Discharge Mixing Areas

The discharge mixing area is the cross-sectional size of the contaminant plume as it passes the control plane. It is used in conjunction with the average velocity and porosity to estimate the volume of groundwater which contains radionuclides.

For both the tracer test and the shot, discharge mixing areas were calculated by estimating the transverse width of the resultant plume at the desired distance, and multiplying this value by the thickness of the Culebra. A value of 10.4 m was used for the Culebra thickness, which reflects conditions at the wells used for the tracer test (Cooper and Glanzman, 1971). To calculate the width of a plume at any given point downgradient, the formula

$$W = w_0 + 2\sqrt{2D_t t} \quad (2)$$

was used, where  $W$  is equal to the downstream plume width,  $w_0$  is the initial transverse source width (18 m for the shot-related plume, 55 m for the tracer test plume),  $D_t$  is the transverse hydrodynamic dispersion coefficient of the aquifer (assumed to be  $10 \text{ m}^2/\text{yr}$ ), and  $t$  is the time of transport. The two terms in this equation represent the initial source width, and the amount of transverse dispersion and diffusion that occurs during transport to the control plane.

Because USGS-8 (the tracer test injection well) is 918 m west, but only 76 m south of SGZ, and groundwater flow is thought to be due west, it was assumed that the radionuclide plumes from the cavity and the tracer test would overlap in space. Because the tracer test plume has a much larger initial source width than the cavity plume, the cavity plume is assumed to occur within the tracer test plume.

Because the value for  $D_t$  ( $10 \text{ m}^2/\text{yr}$ ) was estimated, a sensitivity analysis was performed to determine how changes in the transverse hydrodynamic dispersion coefficient would alter model results for tritium transport. A value of  $1 \text{ m}^2/\text{yr}$  for  $D_t$  was used in the sensitivity analysis.

### **Distance to Control Plane**

Two scenarios were considered. The first scenario involved transport of radionuclides from the shot point and the tracer test injection well to the western boundary of the drilling exclusion area (T23S, R30E, Section 34) defined by the Gnome monument (Reynolds Electrical and Engineering Co., Inc., 1981). The distance from the cavity to the drilling exclusion boundary along the groundwater flowpath was determined to be 1,250 m, based on a map of the site (DOE, 1982, Figure 1). For material injected during the tracer test, the distance was assumed to be 335 m, based on Cooper's (1963) assertion that the injection well is located 915 m west of SGZ. The second scenario involved solving for the distance at which the peak mean concentration of tritium never exceeds 20,000 pCi/L (the Environmental Protection Agency (EPA) concentration limit for human consumption (U.S. Code of Federal Regulations, 1995)), and thus required transport calculations for a variety of distances, incremented at 1,000-m intervals from SGZ.

### **Correlation Scale**

The correlation scale (also known as the integral scale) is the distance beyond which two measurements of hydraulic conductivity tend to exhibit a weak correlation. A large value suggests a system with a high degree of spatial correlation, and has the net effect of extending the path length of higher conductivity conduits. Hoeksema and Kitanidis (1985) report a range for correlation scales of transmissivity in consolidated rock aquifers of 1,400 to 44,700 m (mean of 17,400 m), but these values refer to aquifer-wide properties, and it has been shown that the correlation scale increases systematically with increasing overall scale. Analysis of correlation and overall scales for a number of well-characterized sites revealed a predictable relationship of the correlation scales being approximately ten percent of the overall scale (Gelhar, 1993).

The correlation scale used for each scenario was 1,500 m. Based on data from the WIPP site presented by Cauffman *et al.* (1990), it was estimated that the correlation scale value lies between 1,500 and 6,000 m. Given the extremely short distances from the shot point and the tracer test injection well to the control plane and the relationship between correlation scale and overall scale described above, the low-end value was used. Because of the uncertainty in this value, a sensitivity analysis was performed to determine how changes in the correlation scale would alter the model results for tritium transport. Values of 3,000, 4,500, and 6,000 m were considered in the sensitivity analysis.

### **Effective Porosity**

An effective porosity of ten percent (0.10) was assumed for the Culebra, based on the average value reported by Cooper and Glanzman (1971). The effective porosity is used with the mean velocity and cross-sectional area to determine the groundwater discharge across the control plane, which in turn is used to convert the contaminant flux into concentrations. The porosity is also used in the calculation of velocity, with a smaller effective porosity resulting in larger groundwater velocities. The uncertainty in effective porosity is incorporated in the overall uncertainty in mean velocity, discussed in the following section.

### **Mean Groundwater Velocity**

The mean groundwater velocity used in the transport calculations was 40.2 m/yr. The mean velocity was calculated from values for aquifer transmissivity, thickness, and effective porosity, in conjunction with the regional hydraulic gradient. The dearth of hydrogeologic data from the Gnome site made the selection of the parameters from which this value was calculated a difficult task.

An analysis of data from the WIPP site and surrounding areas conducted by Pohlmann and Andricevic (1994) suggests that velocity may be significantly lower (8.36 m/yr) than the value chosen for modeling, but a conservative estimate of velocity based on data from the Gnome site suggests that velocity may be as high as 65.7 m/yr. These values were used as bounding conditions for the sensitivity analysis, but are not intended to represent "best case" or "worst case" scenarios.

Only two measurements of the transmissivity of the Culebra at the Gnome site have been reported (43.6 m<sup>2</sup>/d and 49.9 m<sup>2</sup>/d). An average value of the six transmissivity in values measured in Nash Draw (as reported by Cauffman *et al.* (1990)) is 35.9 m<sup>2</sup>/d. With all other values held constant, larger transmissivity values will yield larger velocity values. The value of 43.6 m<sup>2</sup>/d was chosen, in combination with the other parameters discussed below, to produce a mean velocity between the two extremes used in the sensitivity analysis, allowing transport to be modeled for a wide range of velocity values. The upper value (49.9 m<sup>2</sup>/d) was used to compute the extreme high velocity for the sensitivity analysis.

Aquifer thickness at the Gnome site is reported as 8.5 m (Atomic Energy Commission, 1962; Gard, 1968) and 9.1 m (Gardner and Sigalove, 1970; Cooper and Glanzman, 1971; Cooper, 1962a). For the mean velocity determination, the value of 9.1 m was selected for use in calculating hydraulic conductivity from the chosen transmissivity value. For calculating the extreme high velocity for use

in the sensitivity analysis, a value of 8 m was arbitrarily selected. Aquifer thickness appears to increase from east to west, as evidenced by the fact that at the WIPP site, the Culebra is typically between 6 and 8 m thick (Cauffman *et al.*, 1990), but west of the Gnome site at wells USGS-4 and USGS-8, it is 10.4 m thick (Cooper and Glanzman, 1971), thus, it is likely that aquifer thickness increases in the direction of groundwater flow.

An effective porosity of 0.10 (Cooper and Glanzman, 1971) was used in the mean velocity calculation. This value is the average of two values (0.078 and 0.111) determined from laboratory analysis of core samples, the only such analysis reported for effective (as opposed to total) porosity. The low value of 0.078 was used to calculate the extreme high velocity for the sensitivity analysis.

A hydraulic gradient of  $2.28 \times 10^{-3}$  (Cooper and Glanzman, 1971) was selected. Although Cooper (1962a) reports the regional hydraulic gradient as varying between  $2.27 \times 10^{-3}$  and  $2.84 \times 10^{-3}$ , analysis of the regional potentiometric surface map presented by Cooper and Glanzman (1971, Plate 1) indicates that the gradient may actually range from  $1.5 \times 10^{-3}$  to  $2.84 \times 10^{-3}$ . Pohl and Pohlmann (1996, in press) suggest that the gradient in the immediate environs of the site may be as low as  $4.2 \times 10^{-4}$ , but the scenarios examined in this report support the use of a more regional gradient value. A mid-range gradient from the values suggested by the potentiometric surface map of Cooper and Glanzman (1971) was chosen ( $2.28 \times 10^{-3}$ ), so as to yield a mid-range velocity value. Because this value appears to be the most reasonable estimate of the gradient along the hypothesized migration path, it was also used to compute the extreme high value for the sensitivity analysis.

The solute flux model includes an estimation error in mean velocity to account for uncertainty in the assigned mean velocity value due to uncertainties in mean effective porosity, mean hydraulic conductivity, and mean hydraulic gradient. The lack of data did not allow calculation of these uncertainties at the Gnome site. Instead, sensitivity analysis for the velocity value was used to examine the effects resulting from an estimation error. It is important to stress that the sensitivity analysis addresses the uncertainty in the mean velocity. The range of velocities in the flow field is incorporated through the spatial variability in hydraulic conductivity and would be expected to be much larger than the uncertainty in the mean. It should also be noted that the "extreme values" selected for use in the sensitivity analyses are not intended to represent "best case" or "worst case" values.

### **Spatial Variability in Hydraulic Conductivity**

It is known that hydraulic conductivity varies through space due to geologic variability. The variability in  $K$  creates flowpaths with both higher and lower mean velocities than those calculated using the mean  $K$ , and results in spreading of a contaminant plume along the direction of flow. The spreading is noted at the control plane as early arrivals in advance of the bulk of the contaminant mass, and a "tail" of trailing arrivals behind the bulk of the mass. The early arrivals caused by spatial variability in hydraulic conductivity are particularly important when considering transport of a decaying solute such as tritium because the mass of contaminant decreases with time. A large variance allows more variation in  $K$  about the mean value, and thus results in a distribution of



velocities that can include much faster flowpaths than the mean. A lower variance restricts the spreading about the mean.

A value of 2.9 was used for the variance in the natural logarithm of hydraulic conductivity ( $\ln K$ ) (Andricevic and Cvetkovic, 1996). This value is based on data from the WIPP site reported by Cauffman *et al.* (1990). After the initial variance ( $\sigma^2 \ln K$ ) of 4.75 was calculated from the data, it was adjusted to incorporate an estimated value for the nugget effect (1.85) to arrive at the variance used in this study (Andricevic and Cvetkovic, 1996). Because of the uncertainty in the variance value, a sensitivity analysis was performed to determine how changes in the variance would alter the model results for tritium transport. Values of 4.5 and 6.0 were considered for the sensitivity analysis.

## RESULTS

A schematic representation of the hypothesized migration pathways for radionuclides to the drilling exclusion boundary is given in Figure 5. A westward flow direction is assumed, based on the potentiometric surface map provided by Cooper and Glanzman (1971). Figure 6 shows the mean concentration of tritium and mean concentration plus two standard deviations at the western edge of the drilling exclusion boundary, 1,250 m west of SGZ. It shows that the tracer test produces a high concentration of tritium almost immediately, with levels declining rapidly until the arrival of the plume from the nuclear test. The nuclear test plume causes concentrations higher than those resulting from the tracer test, and due to the long-term release, levels are slower to decline. According to this scenario, tritium concentration at the drilling exclusion boundary could exceed 20,000 pCi/L from 1963 through 2035. Considering the mean concentration plus two standard deviations to yield a 95 percent confidence level, concentration at the drilling exclusion boundary could be as high as 20,000 pCi/L through 2068.

Following the initial spike in 1963, the peak mean tritium concentration at the drilling exclusion boundary occurs in 1987 (24 years after the Gnome shot) due to migration of material from the nuclear shot. The peak values for the other nuclides considered to be non-sorbing,  $^{36}\text{Cl}$ ,  $^{99}\text{Tc}$ ,  $^{98}\text{Tc}$ , and  $^{129}\text{I}$  occur two years later than the shot-related tritium peak, as a result of having much longer half-lives than tritium. The peak mean concentration of  $^{36}\text{Cl}$  is 6,400 pCi/L (Figure 7a), while  $^{99}\text{Tc}$  peaks at just under 1,000 pCi/L (Figure 7b),  $^{129}\text{I}$  peaks at 6.4 pCi/L and  $^{98}\text{Tc}$  peaks at  $1.8 \times 10^{-4}$  pCi/L (Table 4).

The transport of the sorbing species is substantially slower than that of tritium, as evidenced by the later occurrence of the peak mean concentration at the drilling exclusion boundary.  $^{90}\text{Sr}$  has an early, low peak (28,000 pCi/L) passing by the drilling exclusion boundary due to the tracer test (Figure 8), followed by a larger release of mass when the shot materials are predicted to arrive in 2009 (peak of 76,500 pCi/L).  $^{137}\text{Cs}$  is also migrating from both the tracer test and nuclear shot, but its much larger  $K_d$ , relative to  $^{90}\text{Sr}$  and  $^3\text{H}$ , causes the plumes from the two sources to overlap more. The peak due solely to the tracer test arrives at the boundary in 2049 at a concentration of 5 pCi/L, while the combined peak arrives in 2056 at a concentration of 6.5 pCi/L. With the smaller initial

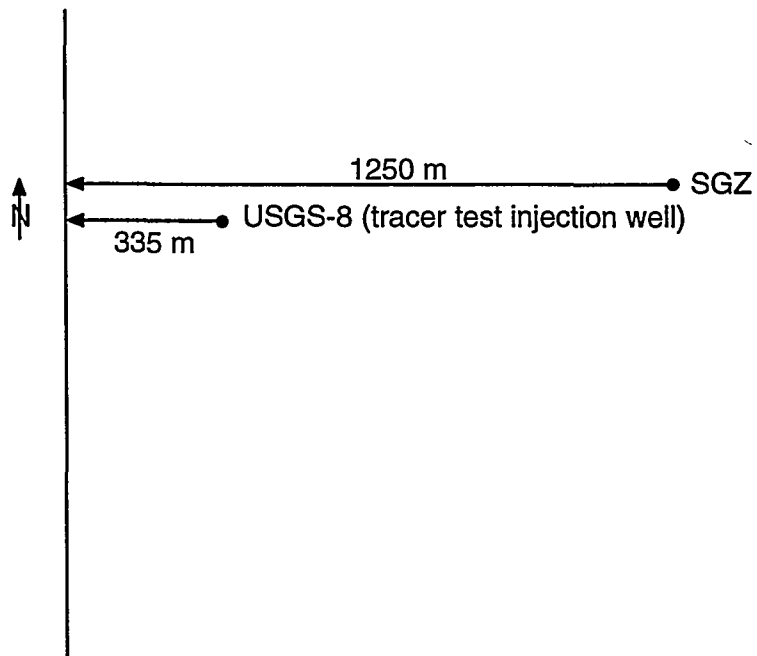


Figure 5. Detail of T23S, R30E, Section 34 showing hypothesized migration paths to the drilling exclusion boundary.

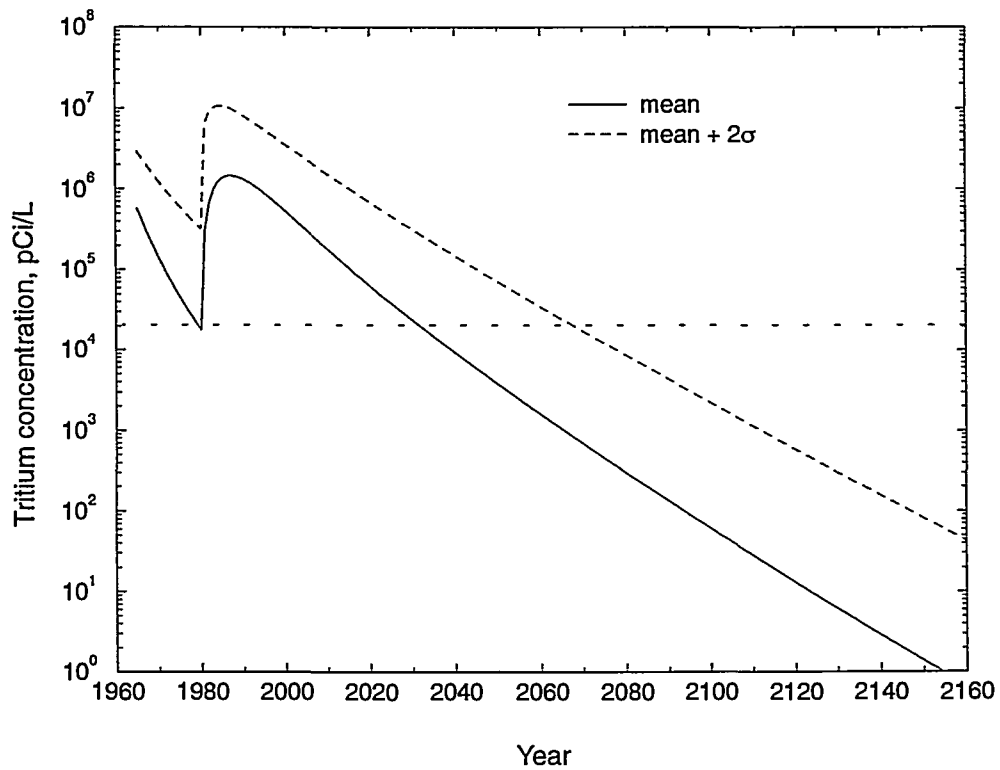


Figure 6. Modeled tritium concentrations at the drilling exclusion boundary resulting from the Gnome shot and tracer test. Dashed line indicates the EPA maximum concentration for human consumption (20,000 pCi/L).

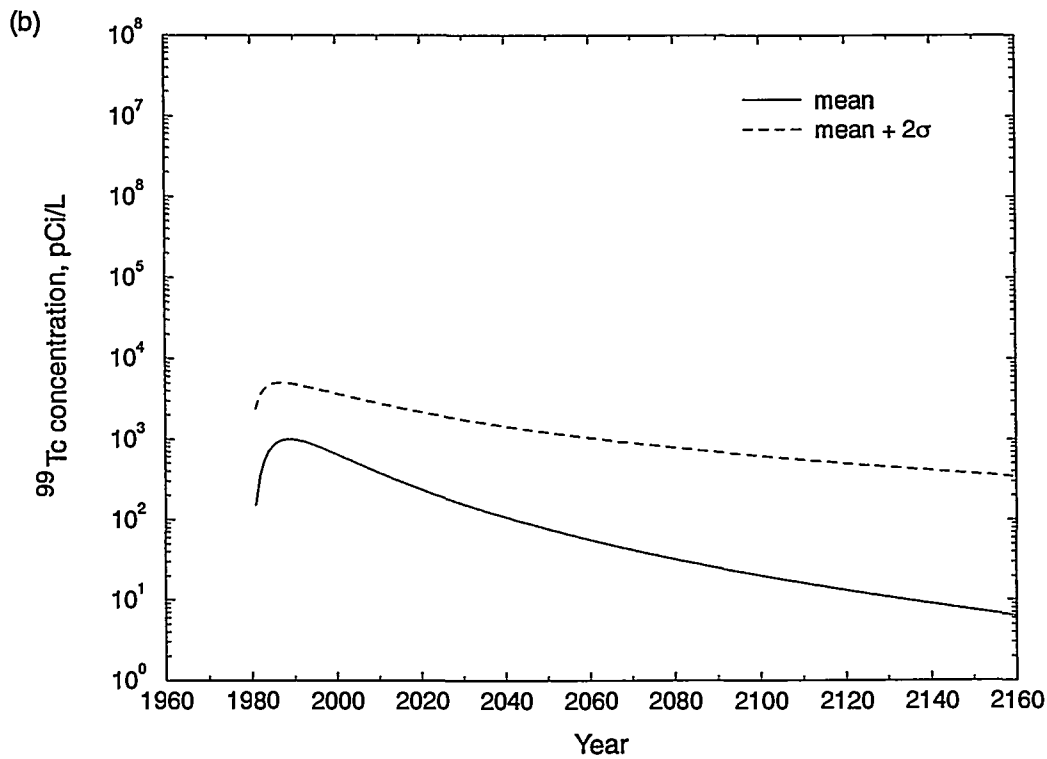
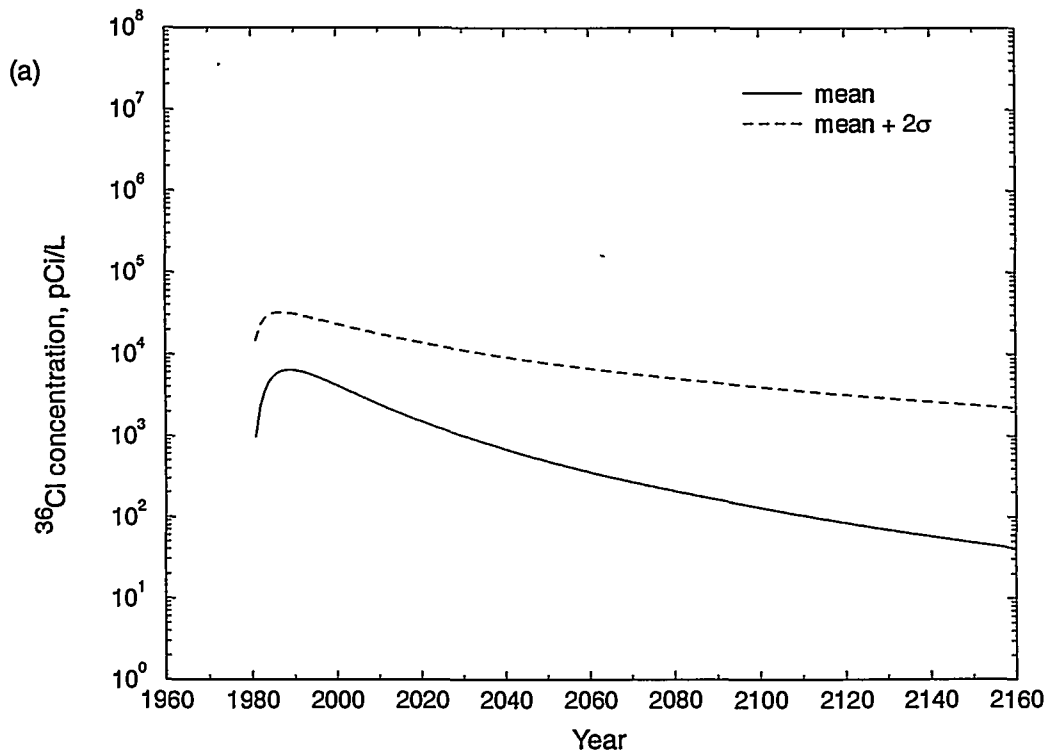


Figure 7. (a) Modeled concentration of  $^{36}\text{Cl}$  from the nuclear shot at the drilling exclusion boundary; and (b) Modeled concentration of  $^{99}\text{Tc}$  from the nuclear shot at the drilling exclusion boundary.

masses and large  $K_d$  values, the other sorbing nuclides with  $K_d$  data (Cs and Eu isotopes) all have modeled peak mean concentrations at the boundary of  $10^{-10}$  pCi/L or less (Table 4).

TABLE 4. RESULTS OF GROUNDWATER TRANSPORT CALCULATIONS FOR NUCLIDES WITH SORPTION INFORMATION. The concentrations presented are the peak values in the mean breakthrough curves at the Gnome site boundary. For reference, nuclide concentrations causing a 4 mrem/yr dose rate per 40 CFR 141.16 (EPA, 1976) and their required detection limits per 40 CFR 141.25, are also presented.

Nuclide	Peak Mean Concentration at the Boundary (pCi/L)	Peak Mean Concentration Plus $2\sigma$ (pCi/L)	Time of Arrival of Peak Mean Concentration at Boundary (yr after 1961)	Concentration causing 4 mrem/yr dose (pCi/L)	Detection limit required in 40 CFR 141.25 (pCi/L)
$^3\text{H}$	$1.9 \times 10^6$	$9.96 \times 10^6$	24	$2.0 \times 10^4$	$1.0 \times 10^3$
$^{36}\text{Cl}$	$6.4 \times 10^3$	$3.2 \times 10^4$	28	$7.0 \times 10^2$	$7.0 \times 10^1$ *
$^{90}\text{Sr}$	$7.7 \times 10^4$	$1.2 \times 10^6$	48	$8.0 \times 10^0$	$2.0 \times 10^0$
$^{98}\text{Tc}$	$1.8 \times 10^{-4}$	$9.0 \times 10^{-4}$	28	NA	NA
$^{99}\text{Tc}$	$1.0 \times 10^3$	$5.0 \times 10^3$	28	$9.0 \times 10^2$	$9.0 \times 10^1$ *
$^{129}\text{I}$	$6.4 \times 10^0$	$3.2 \times 10^1$	28	$1.0 \times 10^0$	$1.0 \times 10^{-1}$ *
$^{134}\text{Cs}$	$1.1 \times 10^{-10}$	$1.8 \times 10^{-5}$	36	$2.0 \times 10^4$	$1.0 \times 10^1$
$^{135}\text{Cs}$	$1.1 \times 10^{-12}$	$1.4 \times 10^{-10}$	6200	$9.0 \times 10^2$	$9.0 \times 10^1$ *
$^{137}\text{Cs}$	$6.5 \times 10^0$	$3.2 \times 10^3$	95	$2.0 \times 10^2$	$2.0 \times 10^1$ *
$^{152}\text{Eu}$	$1.2 \times 10^{-12}$	$8.0 \times 10^{-5}$	140	$6.0 \times 10^1$	$6.0 \times 10^0$ *
$^{154}\text{Eu}$	$1.0 \times 10^{-14}$	$2.4 \times 10^{-6}$	100	$2.0 \times 10^2$	$2.0 \times 10^1$ *
$^{155}\text{Eu}$	$3.0 \times 10^{-15}$	$4.0 \times 10^{-6}$	71	$6.0 \times 10^2$	$6.0 \times 10^1$ *

NA = 168-hour data not available in NBS Handbook 69 (U.S. Dept. of Commerce, 1963) for calculating EPA maximum contaminant level per 40 CFR 141.16

\* = calculated based on 1/10 of applicable limit in 40 CFR 141.16, as described in 40 CFR 141.25

The majority of the radionuclides produced by the Gnome test (Table 2) have no sorption data available for interaction with the Culebra Dolomite. Transport calculations were performed for these nuclides without considering any sorption, though some of these chemical species can be expected to sorb strongly. Despite this conservative assumption, many of these radionuclides are predicted to cross the site boundary in very low concentrations (Table 5) due to either small initial masses or rapid decay. Nuclides in this group that are modeled to cross the boundary with concentrations greater than the EPA-required detection limit are  $^{106}\text{Ru}$ ,  $^{113\text{m}}\text{Cd}$ ,  $^{125}\text{Sb}$ ,  $^{147}\text{Pm}$ , and  $^{151}\text{Sm}$ , but it must be remembered that no sorption was included in the calculations.

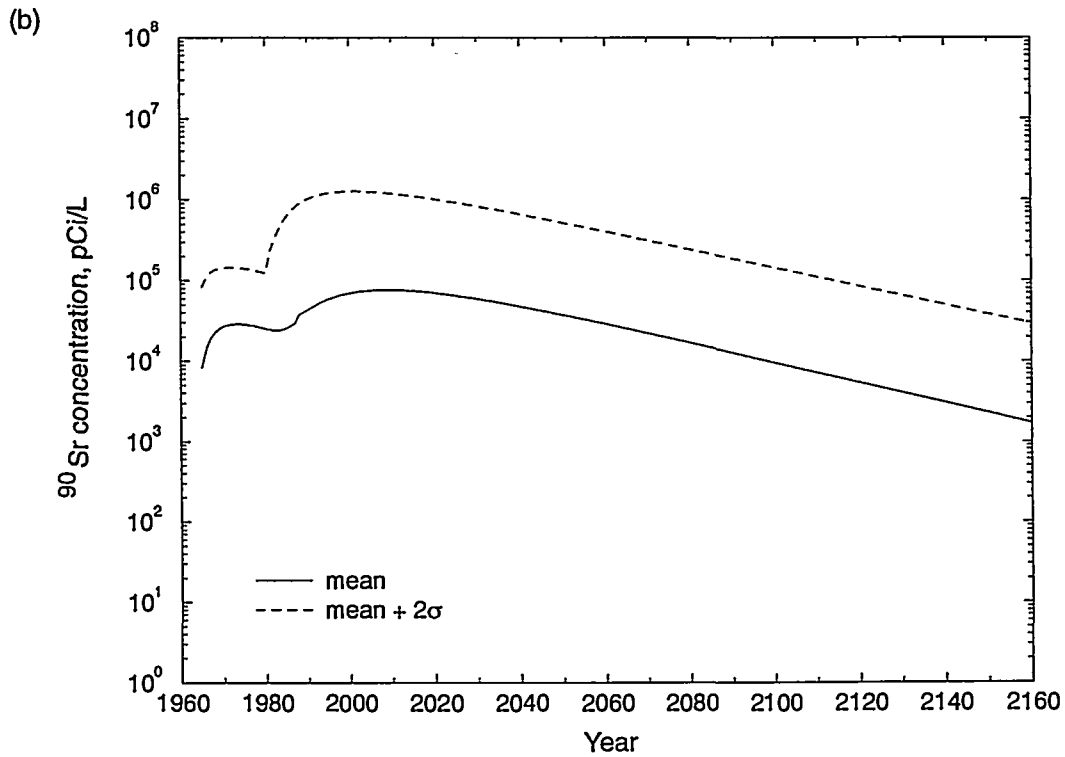
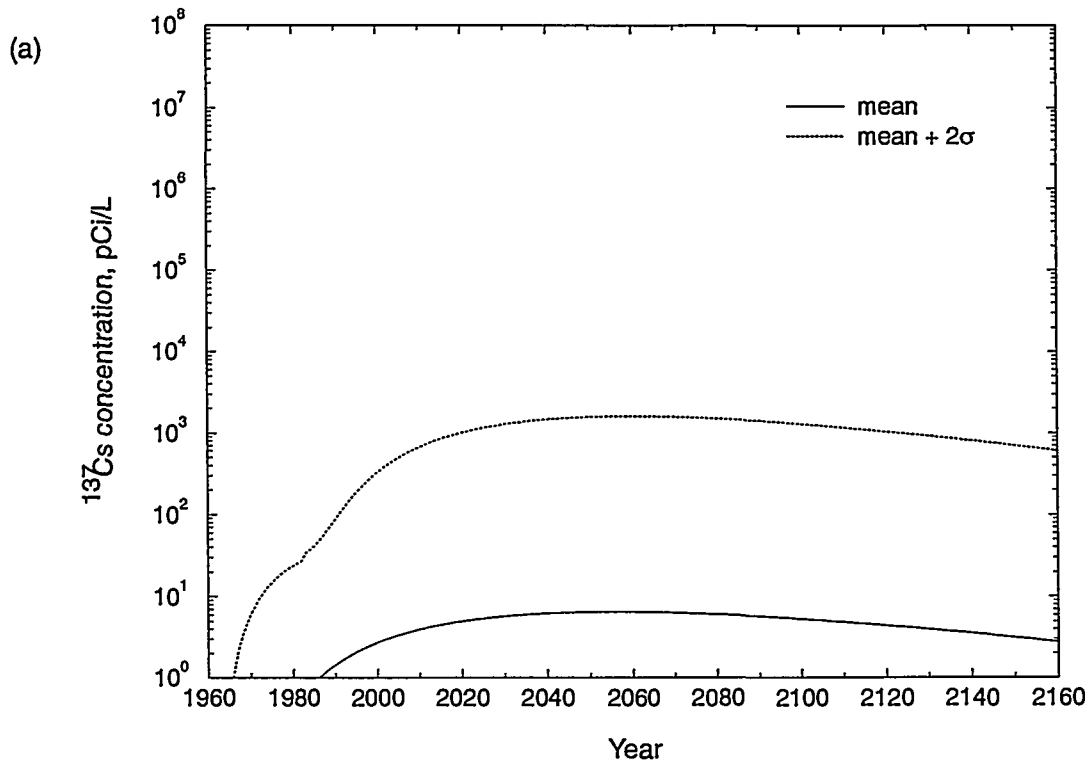


Figure 8. (a) Modeled concentration of  $^{137}\text{Cs}$  from the nuclear shot and tracer test at the drilling exclusion boundary; and (b) Modeled concentration of  $^{90}\text{Sr}$  from the nuclear shot and tracer test at the drilling exclusion boundary.

TABLE 5. RESULTS OF GROUNDWATER TRANSPORT CALCULATIONS FOR NUCLIDES WITHOUT SORPTION INFORMATION. No retardation was assumed for the calculations, though many of these nuclides are expected to be strongly sorbing or be in insoluble form. The concentrations presented are the peak values in the mean breakthrough curves at the Gnome site boundary. For reference, nuclide concentrations causing a 4 mrem/yr dose rate per 40 CFR 141.16 (EPA, 1976) and their required detection limits per 40 CFR 141.25, are also presented.

Nuclide	Peak Mean Concentration at the Boundary (pCi/L)	Peak Mean Concentration Plus 2 $\sigma$ (pCi/L)	Time of Arrival of Peak Mean Concentration at Boundary (yr after 1961)	Concentration causing 4 mrem/yr dose (pCi/L)	Detection limit required in 40 CFR 141.25* (pCi/L)
<sup>14</sup> C	5.6 x 10 <sup>-1</sup>	2.8 x 10 <sup>0</sup>	28	2.0 x 10 <sup>3</sup>	2.0 x 10 <sup>2</sup>
<sup>22</sup> Na	4.6 x 10 <sup>-2</sup>	2.9 x 10 <sup>-1</sup>	23	4.0 x 10 <sup>2</sup>	4.0 x 10 <sup>1</sup>
<sup>40</sup> K	4.4 x 10 <sup>-3</sup>	2.2 x 10 <sup>-2</sup>	28	NA	NA
<sup>41</sup> Ca	9.6 x 10 <sup>0</sup>	4.8 x 10 <sup>1</sup>	28	NA	NA
<sup>45</sup> Ca	2.2 x 10 <sup>-9</sup>	2.6 x 10 <sup>-8</sup>	21	1.0 x 10 <sup>1</sup>	1.0 x 10 <sup>0</sup>
<sup>54</sup> Mn	2.2 x 10 <sup>-8</sup>	1.8 x 10 <sup>-7</sup>	22	3.0 x 10 <sup>2</sup>	3.0 x 10 <sup>1</sup>
<sup>55</sup> Fe	5.6 x 10 <sup>-1</sup>	3.6 x 10 <sup>0</sup>	23	2.0 x 10 <sup>3</sup>	2.0 x 10 <sup>2</sup>
<sup>57</sup> Co	6.6 x 10 <sup>-11</sup>	6.9 x 10 <sup>-10</sup>	21	1.0 x 10 <sup>3</sup>	1.0 x 10 <sup>2</sup>
<sup>60</sup> Co	1.0 x 10 <sup>-1</sup>	5.4 x 10 <sup>-1</sup>	25	1.0 x 10 <sup>2</sup>	1.0 x 10 <sup>1</sup>
<sup>63</sup> Ni	5.4 x 10 <sup>-1</sup>	2.6 x 10 <sup>0</sup>	28	5.0 x 10 <sup>1</sup>	5.0 x 10 <sup>0</sup>
<sup>65</sup> Zn	8.5 x 10 <sup>-9</sup>	9.1 x 10 <sup>-8</sup>	21	3.0 x 10 <sup>2</sup>	3.0 x 10 <sup>1</sup>
<sup>87</sup> Rb	8.4 x 10 <sup>-4</sup>	4.2 x 10 <sup>-3</sup>	28	3.0 x 10 <sup>2</sup>	3.0 x 10 <sup>1</sup>
<sup>94</sup> Nb	8.0 x 10 <sup>-2</sup>	4.0 x 10 <sup>-1</sup>	28	NA	NA
<sup>106</sup> Ru	6.8 x 10 <sup>1</sup>	5.4 x 10 <sup>2</sup>	22	3.0 x 10 <sup>1</sup>	3.0 x 10 <sup>0</sup>
<sup>102</sup> Rh	4.8 x 10 <sup>-2</sup>	2.7 x 10 <sup>-1</sup>	24	NA	NA
<sup>107</sup> Pd	1.5 x 10 <sup>-2</sup>	7.3 x 10 <sup>-2</sup>	28	NA	NA
<sup>110m</sup> Ag	3.6 x 10 <sup>-5</sup>	3.8 x 10 <sup>-4</sup>	21	9.0 x 10 <sup>1</sup>	9.0 x 10 <sup>0</sup>
<sup>113m</sup> Cd	4.1 x 10 <sup>1</sup>	2.1 x 10 <sup>2</sup>	26	NA	NA
<sup>115</sup> In	3.9 x 10 <sup>-9</sup>	1.9 x 10 <sup>-8</sup>	28	3.0 x 10 <sup>2</sup>	3.0 x 10 <sup>1</sup>
<sup>125</sup> Sb	5.0 x 10 <sup>3</sup>	3.2 x 10 <sup>4</sup>	23	3.0 x 10 <sup>2</sup>	3.0 x 10 <sup>1</sup>
<sup>138</sup> La	1.0 x 10 <sup>-4</sup>	5.0 x 10 <sup>-4</sup>	28	NA	NA
<sup>144</sup> Nd	2.2 x 10 <sup>-8</sup>	1.1 x 10 <sup>-7</sup>	28	1.0 x 10 <sup>2</sup>	1.0 x 10 <sup>1</sup>
<sup>147</sup> Pm	6.2 x 10 <sup>4</sup>	4.0 x 10 <sup>5</sup>	23	6.0 x 10 <sup>2</sup>	6.0 x 10 <sup>1</sup>
<sup>147</sup> Sm	6.0 x 10 <sup>-4</sup>	3.0 x 10 <sup>-3</sup>	28	9.0 x 10 <sup>1</sup>	9.0 x 10 <sup>0</sup>
<sup>151</sup> Sm	2.9 x 10 <sup>5</sup>	1.4 x 10 <sup>6</sup>	28	1.0 x 10 <sup>3</sup>	1.0 x 10 <sup>2</sup>
<sup>153</sup> Gd	2.5 x 10 <sup>-9</sup>	2.7 x 10 <sup>-8</sup>	21	6.0 x 10 <sup>2</sup>	6.0 x 10 <sup>1</sup>
<sup>158</sup> Tb	6.9 x 10 <sup>-1</sup>	3.4 x 10 <sup>0</sup>	28	NA	NA

NA = 168-hour data not available in NBS Handbook 69 (U.S. Dept. of Commerce, 1963) for calculating EPA maximum contaminant level per 40 CFR 141.16

\* = calculated based on 1/10 of applicable limit in 40 CFR 141.16, as described in 40 CFR 141.25

Because the release of shot-produced radionuclides into the Culebra is not a certainty, the results of radionuclide migration from the tracer test alone were also investigated. As shown in

Figure 9, if no plume from the shot were to cross the drilling exclusion boundary, tritium would exceed 20,000 pCi/L at the boundary only through 1984 (although concentrations would continue to exceed that amount west of the boundary). It is also worth noting that if release from the cavity does take place, the time over which release occurs may be higher than the 12 years used in this study. If this were the case, the tritium breakthrough curve resulting from the shot would have a lower peak, but would be slower to decline.

Transport calculations were performed for various distances downgradient from SGZ to determine the location at which the peak mean concentration of tritium from the combined effects of the shot and the tracer test would not exceed 20,000 pCi/L at any time. This point is slightly less than 8 km west of SGZ (Figure 10), and the peak concentration at that distance occurs in 2010.

### SENSITIVITY ANALYSES

As discussed earlier, the lack of hydrogeologic data from the Gnome site could cause large discrepancies between model results and reality. To understand the relative importance of uncertainty in various model parameters, sensitivity analyses were conducted for the correlation scale of hydraulic conductivity, mean groundwater velocity, the variance of hydraulic conductivity, and the transverse hydrodynamic dispersion coefficient. For these hydraulic parameters, mean tritium concentration 8 km west of SGZ was computed to see how it differed from the 20,000-pCi/L value initially predicted. Additional modeling was conducted to approximate the distance from SGZ at which tritium concentrations would not exceed 20,000 pCi/L. The sensitivity of sorption values was analyzed by evaluating  $^{90}\text{Sr}$  and  $^{137}\text{Cs}$  concentrations crossing the site boundary. Although uncertainty exists in the source term, this was not addressed via sensitivity analyses, because it would be difficult to estimate bounding values without using classified data. The sensitivity analyses were conducted by holding all parameters constant, except the one being examined. Possible correlations among parameters were ignored.

Figure 11 shows the results of the sensitivity analysis for the correlation scale. Since 1,500 m was considered the lowest possible value, the correlation scale was increased in 1,500-m increments to 6,000 m, thought to be the highest possible correlation scale for the Culebra. At 8 km from SGZ, increasing values of  $\lambda$  cause increases in tritium concentration, with a  $\lambda$  of 6,000 m producing a mean concentration of 65,650 pCi/L, over three times higher than that predicted for  $\lambda=1500$  m. If a correlation scale of 6,000 m is assumed, model results suggest that peak mean tritium concentration would remain above 20,000 pCi/L to a distance of approximately 12 km west of SGZ.

The results of the sensitivity analysis for mean velocity are shown in Figure 12. Data from the region of halite dissolution in the Gnome/WIPP region (Cauffman *et al.*, 1990) analyzed by Pohlmann and Andricevic (1994) suggest a mean velocity of 8.36 m/yr. This was assumed to be the lowest reasonable velocity for groundwater in the Culebra in the Gnome area. A conservative estimate of the maximum possible velocity was generated by using data from the Gnome site, yielding a value of 65.7 m/yr. If mean velocity is assumed to be 8.36 m/yr, peak mean tritium concentration 8 km west of SGZ would be less than 300 pCi/L, and peak mean concentration would drop below 20,000 pCi/L less than 4 km from SGZ. For the upper velocity of 65.7 m/yr, mean

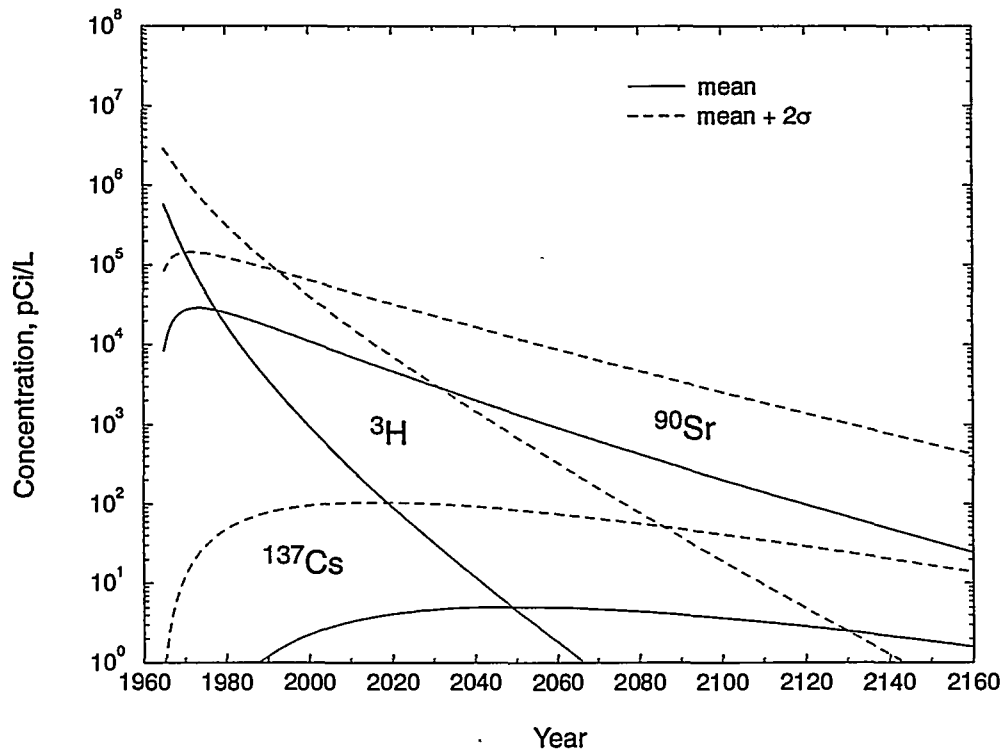


Figure 9. Modeled  $^3\text{H}$ ,  $^{90}\text{Sr}$ , and  $^{137}\text{Cs}$  concentrations at the drilling exclusion boundary resulting from the tracer test only.

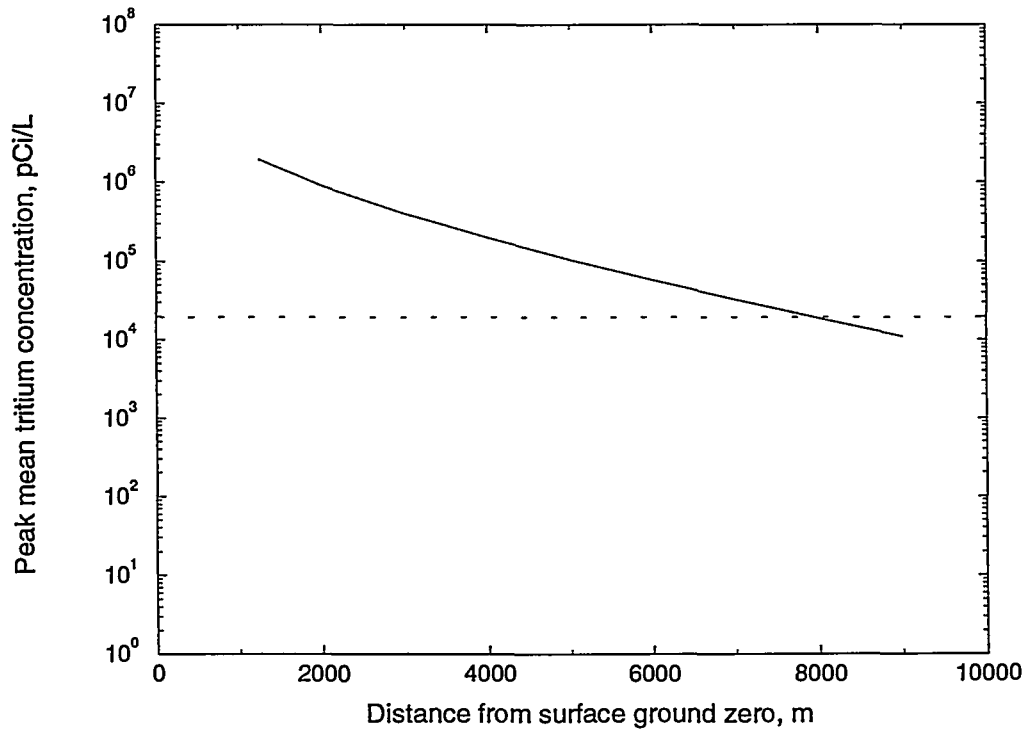


Figure 10. Modeled peak mean tritium concentrations versus distance west of surface ground zero. Dashed line indicates the EPA maximum concentration for human consumption (20,000 pCi/L).



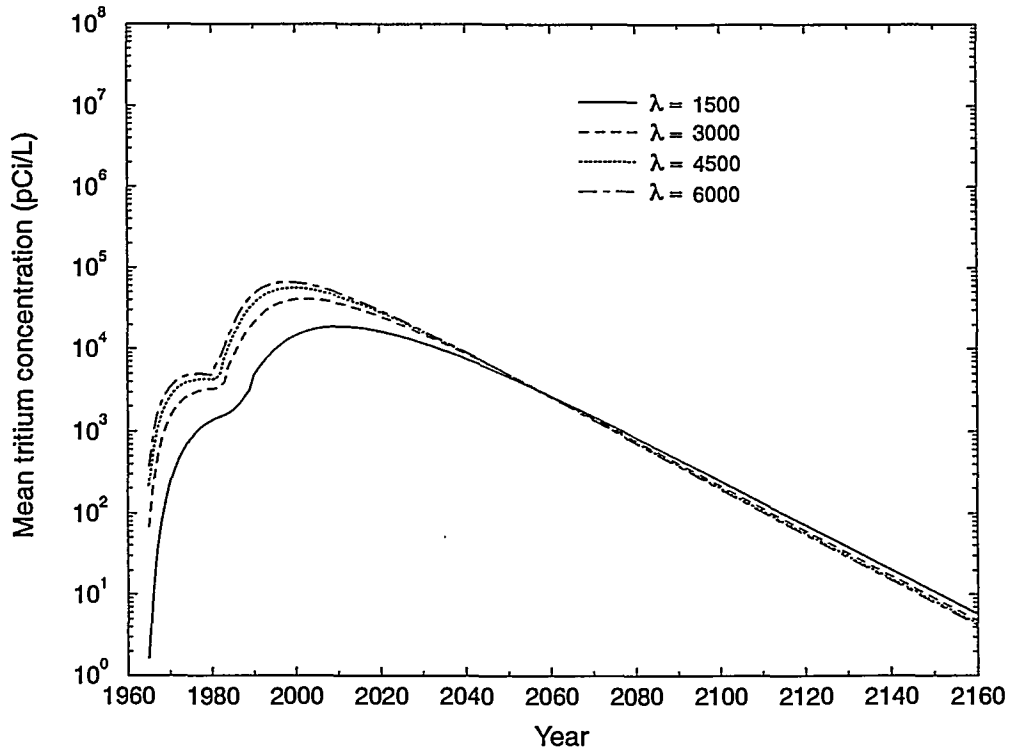


Figure 11. Sensitivity of mean tritium concentration 8 km west of surface ground zero to changes in correlation scale.

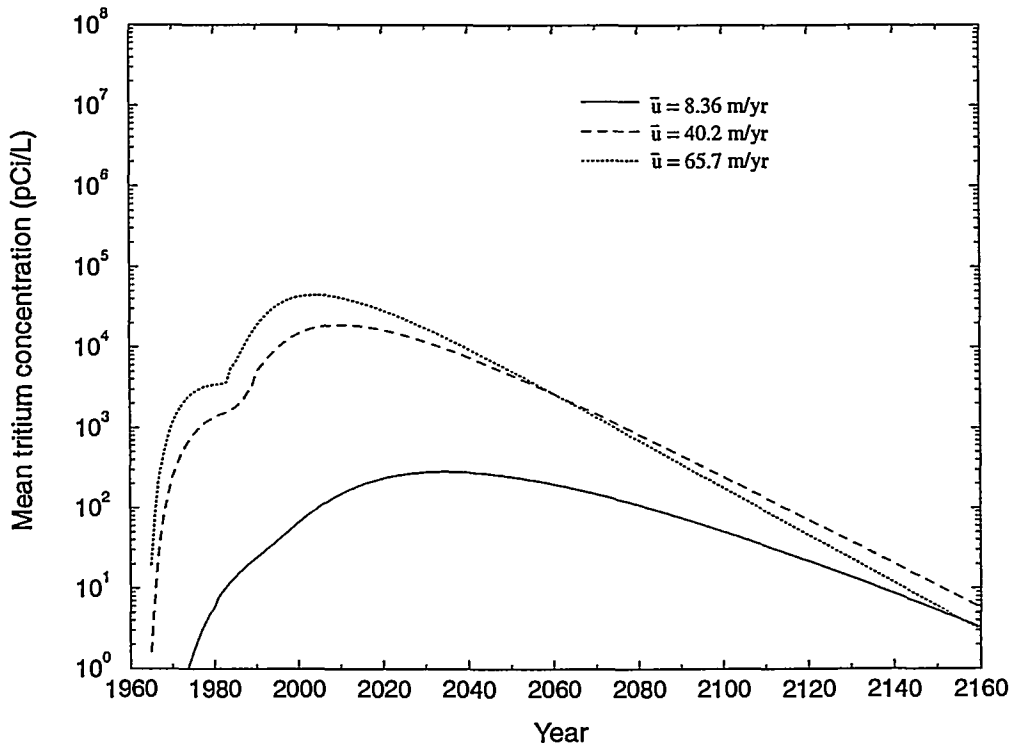


Figure 12. Sensitivity of mean tritium concentration 8 km west of surface ground zero to changes in mean velocity.

concentration 8 km from SGZ would peak at 45,000 pCi/L, and the peak mean concentration would cease to exceed 20,000 pCi/L slightly less than 10 km west of SGZ. This nearly eightfold range in mean velocity values produces a two order of magnitude range in concentration values.

Figure 13 shows the results of the sensitivity analysis for variance. Data from the Gnome site suggest an extremely large variance, but this is probably a result of the small number of data rather than an actual indication of the variance. Nonetheless, variances higher than that used in the initial calculations were selected for the sensitivity analysis. It should be noted that these variances are probably far higher than would be expected were more data available, but the results are still useful, in that they illustrate the effect that error in the variance has on predicted radionuclide concentrations. If a variance of 6.0 is assumed, mean tritium concentration 8 km west of SGZ would peak at 60,200 pCi/L, and would require nearly 11 km to fall below 20,000 pCi/L. This factor of two increase in the variance produces a threefold increase in the predicted concentration. It is also important to note that the solute flux model is an approach based on a first-order approximation of variance, and thus loses accuracy when  $\sigma^2$  is larger than two or three.

The results of the sensitivity analysis for the transverse hydrodynamic dispersion coefficient are shown in Figure 14. The transverse hydrodynamic dispersion coefficient used in this study was estimated from aquifer properties, most notably the fact that fractures are the principal pathways for the transmission of water through the Culebra. Although there is no known information regarding fracture geometry at Gnome, it was assumed that a randomly oriented set of fractures exists, thus allowing for a high transverse dispersivity relative to an aquifer where pore flow or flow through aligned fractures carries most of the water. The high value chosen for  $D_t$  causes the contaminant plume to be larger than it would had a lower value been assumed; spreading the mass over a larger area results in a lower mean concentration. To determine how changes in  $D_t$  affect the model results for tritium concentration, a sensitivity analysis was performed, using the original value of 10 m<sup>2</sup>/yr, and a low value of 1 m<sup>2</sup>/yr. If  $D_t$  is assumed to be 1 m<sup>2</sup>/yr, mean tritium concentration 8 km west of SGZ would peak at 44,200 pCi/L, and would require slightly over 9 km to drop below 20,000 pCi/L. This factor of ten change in  $D_t$  produces a twofold range in modeled concentration values.

Very little information is available on the various attenuation factors that can retard radionuclide transport. The sensitivity of the calculations to the mean sorption coefficient was examined for <sup>90</sup>Sr and <sup>137</sup>Cs by considering the upper and lower bounds measured by Lynch and Dosch (1980) (Table 3) as the mean, and assuming the same variance. The calculated concentrations are quite sensitive to the  $K_d$  used (Figures 15 and 16). For <sup>90</sup>Sr, a factor of two change in the value of  $K_d$  caused a range in peak mean concentration of 48,000 to 130,000 pCi/L. The <sup>137</sup>Cs concentrations show a larger impact due to the much larger range in  $K_d$  values measured by Lynch and Dosch (1980). The sevenfold range in  $K_d$  for <sup>137</sup>Cs causes a two order of magnitude difference in the calculated mean concentration crossing the Gnome boundary (1 pCi/L to 370 pCi/L). Given the sensitivity of the transport calculations to the  $K_d$ , it is extremely important to understand the reliability of the laboratory data on which they are based, the applicability of the laboratory conditions to geochemical conditions in the Culebra, and the natural variation in solubility and  $K_d$  within the aquifer due to geochemical heterogeneity.

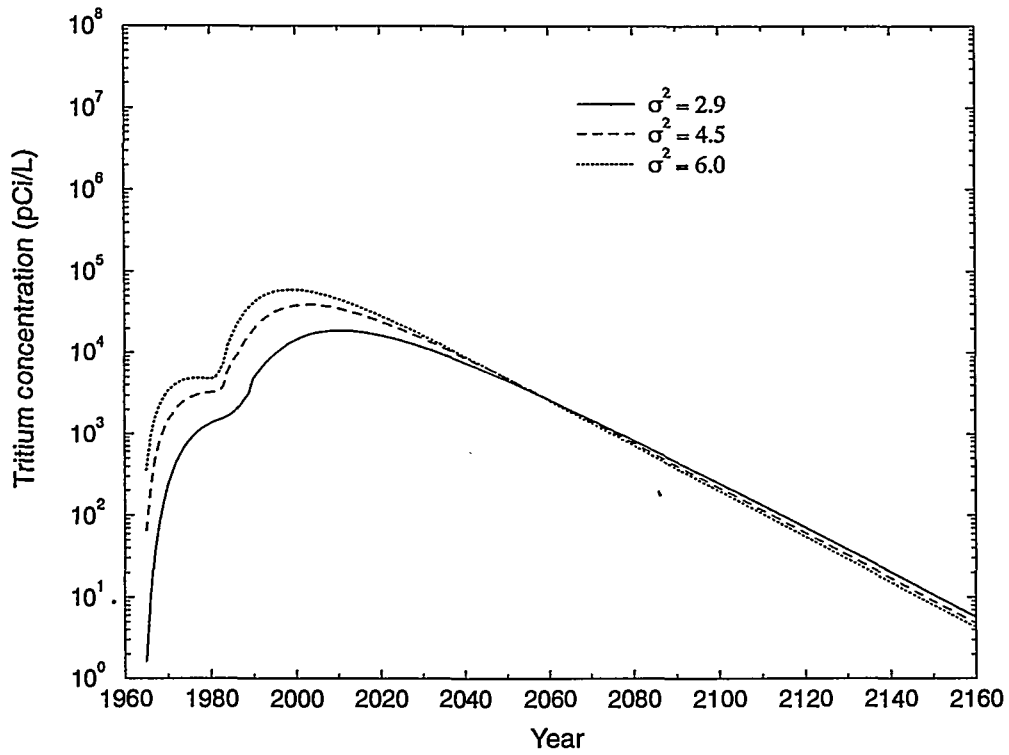


Figure 13. Sensitivity of mean tritium concentration 8 km west of surface ground zero to changes in variance.

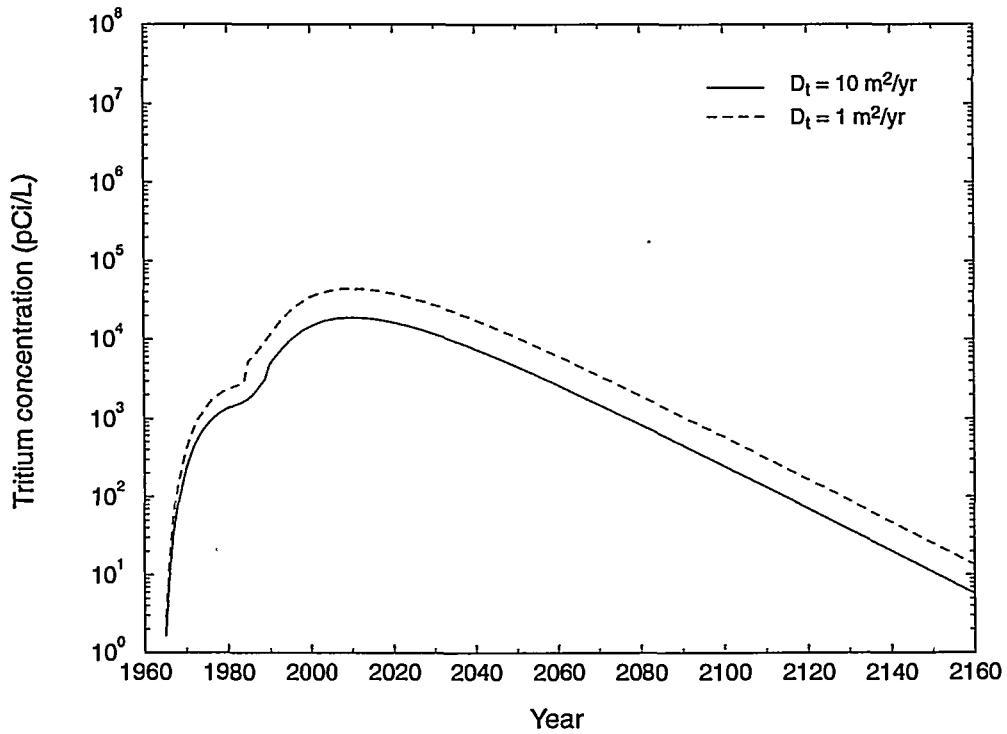


Figure 14. Sensitivity of mean tritium concentration 8 km west of surface ground zero to changes in the hydrodynamic dispersion coefficient.

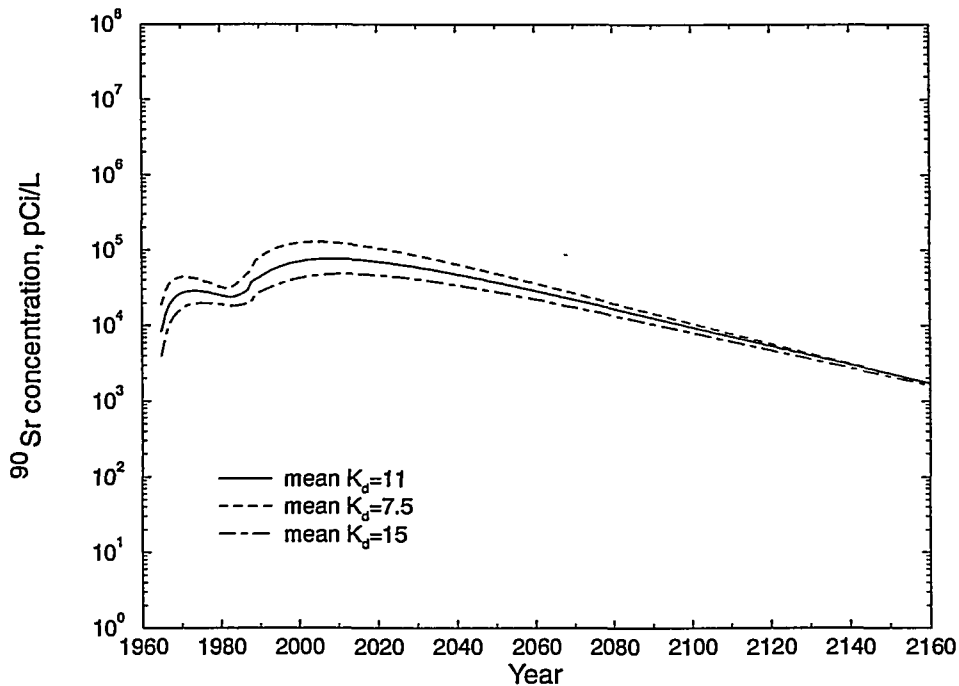


Figure 15. Sensitivity of modeled  $^{90}\text{Sr}$  concentrations crossing the Gnome site boundary to the mean  $K_d$ . The low and high values are based on the lowest and highest laboratory measurements presented by Lynch and Dosch (1980) and shown in Table 3. The value of 11 was the mean based on the range, and in all cases the variance was assumed to be 3.5.

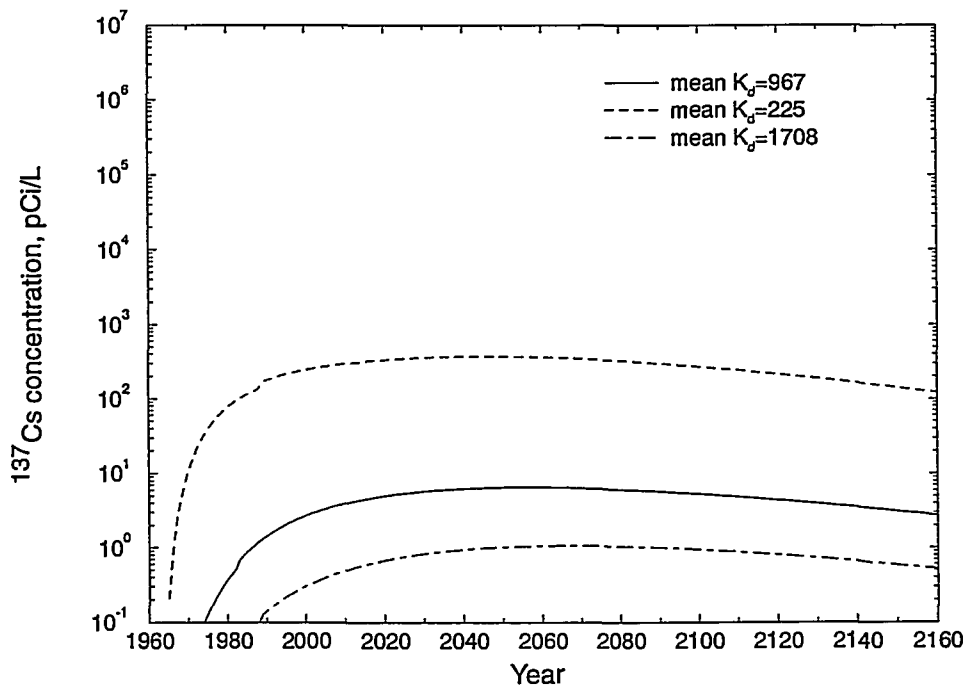


Figure 16. Sensitivity of modeled  $^{137}\text{Cs}$  concentrations crossing the Gnome site boundary to the mean  $K_d$ . The low and high values are based on the lowest and highest laboratory measurements presented by Lynch and Dosch (1980) and shown in Table 3. The value of 967 was the mean based on the range, and in all cases the variance was assumed to be 3.5.

## DISCUSSION

The U.S. Environmental Protection Agency (EPA) promulgated regulations in 1976 regarding radionuclides in community water systems through 40 CFR 141, the Primary Drinking Water Regulations. Part 141.16 describes the maximum contaminant levels for beta particle and photon radioactivity from man-made radionuclides in community water systems. Though no community water systems currently exist downgradient of the Gnome Site, Part 141.16 provides a useful basis of comparison for the radionuclide concentrations calculated in the previous section.

The drinking water regulations actually limit the combined concentration of beta particle and photon radioactivity from man-made radionuclides to that producing less than an annual dose equivalent to the total body or any internal organ of 4 millirem/yr. Thus, the concentration limit for an individual radionuclide is influenced by the presence or absence of other radionuclides. For instance, the average annual concentration of  $^3\text{H}$  assumed to produce a total body dose rate of 4 mrem/yr is 20,000 pCi/L and the concentration of  $^{90}\text{Sr}$  assumed to produce a dose rate of 4 mrem/yr to bone marrow is 8 pCi/L. Those values would be the concentration limits only if either tritium or  $^{90}\text{Sr}$  were the only man-made beta or photon emitter in the water (above detection). If both  $^3\text{H}$  and  $^{90}\text{Sr}$  are present, or if they are present with any other beta or photon emitter, the maximum concentration limits for each will be lower such that the combined dose rate remains below 4 mrem/yr.

The concentration limits where more than one radionuclide is concerned are obviously non-unique. For ease of reference, the radionuclide concentrations calculated for groundwater transport from Gnome are compared to the maximum concentration limit calculated based on that radionuclide being the only one present (Tables 4 and 5). It should be recognized that this is merely for reference, and that the regulated concentration is likely to be lower because more than one radionuclide may be present. It should also be noted that there have been improvements in dose methodology over that promulgated in 40 CFR 141.16 in 1976, and that changes in the drinking water regulations regarding man-made radionuclides are pending. The proposed revision would result in an increase in the concentration calculated to cause a 4 mrem/yr dose rate for most radionuclides (*e.g.*, a proposed change in the maximum concentration of tritium from 20,000 to 90,000 pCi/L) (Stephen Pia, EPA Environmental Monitoring Systems Laboratory, Las Vegas, NV, personal communication). Given the preliminary status of the proposed revisions, all of the maximum contaminant levels referred to here are those in 40 CFR 141.16 as of 1996.

Of the radionuclides with sorption information, five had predicted mean concentrations that exceeded the 4 mrem-based concentration (Table 4). These nuclides were the ones that were assumed to have no transport-retarding properties ( $^3\text{H}$ ,  $^{36}\text{Cl}$ ,  $^{99}\text{Tc}$ ,  $^{129}\text{I}$ ) or weakly sorbing characteristics ( $^{90}\text{Sr}$ ,  $^{99}\text{Tc}$  may also bind weakly to iron and manganese coatings, though no sorption was assumed for these calculations). In the case of both tritium and  $^{90}\text{Sr}$ , having the tracer test as a source in addition to the nuclear shot also contributes to transport. The other long-lived radionuclide included in the tracer test,  $^{137}\text{Cs}$ , is predicted to cross the boundary at a mean concentration of 6.5 pCi/L, well below the 4 mrem-based concentration of 200 pCi/L. However, the

95% confidence interval on the  $^{137}\text{Cs}$  concentration is greater than 3,000 pCi/L, and  $^{137}\text{Cs}$  may contribute toward the total 4 mrem/yr limit. The other radionuclides on Table 4 have peak mean concentrations crossing the Gnome boundary many orders of magnitude below the 4 mrem-based concentration, as well as below the detection limits required by EPA. The low concentrations are a result of either relatively small initial masses combined with decay, and/or strongly sorbing properties indicated by the sparse laboratory data.

Many of the radionuclides listed in Table 2 as being present due to the Gnome shot had no sorption data for reactions with the Culebra Dolomite. Transport calculations were performed for these radionuclides as well, but no retardation was assumed, though many of these nuclides can reasonably be expected to sorb onto solid surfaces. The majority of these nuclides have peak mean concentrations crossing the Gnome boundary less than both the 4 mrem-based concentration and the detection limit (Table 5), even without considering retardation due to sorption. Four nuclides on Table 5 exceed the 4 mrem-based concentrations. The two that exceed by the largest margins,  $^{147}\text{Pm}$  and  $^{151}\text{Sm}$ , can reasonably be expected to have strongly sorbing properties, based on the fission product  $K_d$  values reported in Table 3, and the predicted concentrations would be substantially reduced by including sorption. The potential sorption behavior of  $^{106}\text{Ru}$  and  $^{125}\text{Sb}$  is less clear and depends on many factors, such as the nuclide's oxidation state. As with  $^{99}\text{Tc}$ ,  $^{125}\text{Sb}$  may bind on iron and manganese coatings. Radioactive decay, combined with the relatively short half-life of these four nuclides, results in sorption being a significant remediating process, requiring experimental data to justify sorption values assumed in future calculations.

The calculated peak mean concentrations presented in Tables 4 and 5 all consider transport from the Gnome nuclear cavity as well as the tracer test. As described in the section on "Release Scenarios," it is not known if any release will ever occur from the Gnome nuclear test. The hydrogeologic environment surrounding the nuclear cavity (bedded salt) is highly favorable for containing contaminants, as evidenced by the plans to dispose of nuclear waste in the Salado Formation at the WIPP Site. The cavity release scenario considered here is only possible through a system failure caused by improperly plugged boreholes. If such a failure has not occurred, the only source of groundwater contamination is the tracer test. Considering the tracer test alone as the only known source of contamination to the Culebra Dolomite, calculated mean concentrations for tritium and  $^{90}\text{Sr}$  (680,000 pCi/L for the peak mean tritium concentration crossing the site boundary, approximately 29,000 pCi/L for  $^{90}\text{Sr}$ ) still exceed the 4 mrem-based concentration limits. The peak mean concentration of  $^{137}\text{Cs}$  is just over 5 pCi/L due to the tracer test alone, below the 200 pCi/L limit, as it is for the combined tracer test-nuclear shot scenario. Thus, the results suggest that even without the release of radionuclides from the Gnome cavity to the Culebra, concentrations of  $^3\text{H}$  and  $^{90}\text{Sr}$  greater than drinking water standards may be present beyond the current drilling exclusion boundary. If these radionuclides do migrate from the cavity into the Culebra Dolomite, model results indicate that concentrations outside the drilling exclusion boundary will exceed regulatory guidelines by a greater margin, and will remain above human consumption limits for a longer period of time. In addition, because the EPA drinking water regulations require annual dose equivalents to

be added for all nuclides, the presence of materials from the cavity other than  $^3\text{H}$  and  $^{90}\text{Sr}$  would further exacerbate exceedence levels.

These results are based on available data, which are extremely sparse. If the available values for various transport parameters are not an accurate representation of conditions at the site, the results presented here could deviate significantly from reality. In addition, many of the results presented in this report are based on the conservative assumption that radionuclides from the cavity began migrating through the Culebra in 1979. This assumption can neither be verified nor refuted without further hydrogeologic investigation. The reader should also bear in mind the uncertainties that exist in both the hypothesized release pathway and the source term used in this report.

Monitoring of tritium levels in well USGS-8 by the EPA (EPA, 1992) shows levels far below concentrations predicted using the combined nuclear-test release and tracer-test migration scenario hypothesized for this study, but the values are higher than those predicted to result solely from the tracer test migration alone. There are two possible explanations for these discrepancies: either the aquifer parameters are significantly different from those assumed here, or the release scenarios are incorrectly modeled. Uncertainty in the aquifer parameters is discussed below. In addition to the fundamental uncertainty regarding whether or not a release can occur from the nuclear shot cavity, there are uncertainties as to the release function that affect the timing and magnitude of introduction of radionuclides into the aquifer. The tracer test scenario has uncertainties of its own, regarding the pre-test injection of tritium and details of test conduct. The tracer test data were used to constrain migration estimates of the tracer plume, and the results are reported separately (Pohll and Pohlmann, 1996 (in press)). The EPA monitoring data serve as a reminder that the assessment presented here is preliminary in nature and will be refined by acquiring additional site data.

Aquifer parameter values used in the sensitivity analysis were chosen based on available data for the Gnome site, and comparing the changes in concentration over the ranges used provides site-specific insight as to which parameters have the greatest effect on model results. The sensitivity analyses indicate that given the ranges used for the hydraulic transport parameters, changes in mean velocity (8.36 to 65.7 m/yr) cause more variation in model results (300 pCi/L to 45,000 pCi/L 8 km west of SGZ) than changes in either the correlation scale (1,500 to 6,000 m yielding values from 20,000 pCi/L to 65,650 pCi/L), the variance ( $\ln K$ ) (2.9 to 6.0 yielding values from 20,000 pCi/L to 60,200 pCi/L), or the transverse hydrodynamic dispersion coefficient (1 to 10  $\text{m}^2/\text{yr}$  yielding values from 20,000 pCi/L to 44,200 pCi/L).

For radionuclides with sorbing properties, model results are also sensitive to the sorption coefficient used. Not only are sorption data very sparse for Gnome, but variations in sorption and other attenuation processes (mineral precipitation as controlled by solubility) can be very large *in situ*, depending on geochemical conditions. Thus, if a greater understanding of radionuclide transport from the Gnome site is desired, a more accurate value for velocity along the migration path is the most important hydraulic information to obtain, while data on sorption are important for sorbing species.

It is important to note that the sensitivity analyses were conducted by holding all parameters constant, except the one being examined. If the value for any parameter differs from the value used in the sensitivity analyses for the remaining parameters, then the relative importance of those parameters could be different than that suggested here.

Groundwater velocity is typically calculated based on values for aquifer transmissivity, thickness, and effective porosity, as well as the regional hydraulic gradient. A series of velocity calculations was performed using the currently known ranges of these parameters at the Gnome site (transmissivity of 43.6 to 49.9 m<sup>2</sup>/d, thickness of 8 to 10 m, effective porosity of 0.078 to 0.111, and hydraulic gradient of  $1.5 \times 10^{-3}$  to  $2.84 \times 10^{-3}$ ), while holding all other values constant. The results of these calculations indicate that the range in the hydraulic gradient produced the greatest range of velocity values, followed by the ranges in effective porosity, aquifer thickness, and transmissivity.

The results presented in this study differ somewhat from those presented by Pohlmann and Andricevic (1994). The main reason for the discrepancy is that, in light of the extreme uncertainty regarding radionuclide release from the cavity and the hydrogeologic properties of the Culebra Dolomite, conservative assumptions were used in this study to generate a scenario for transport from both the nuclear shot and the tracer test, while Pohlmann and Andricevic (1994) used data from the WIPP site in order to model a scenario for radionuclide transport from the tracer test alone. The results of both this study and that of Pohlmann and Andricevic (1994) make clear the need for the collection of data regarding the properties of the aquifer, especially groundwater velocity and estimates of the interactions of selected radionuclides with the Culebra Dolomite.

## CONCLUSIONS

The results of this study suggest that radionuclides from the Gnome shot and tracer test may be present in groundwater in the Culebra in excess of EPA human consumption guidelines beyond the current drilling exclusion boundary. The transport analysis is based on extremely sparse data, and as a result, may differ greatly from the actual conditions. These results are meant to serve as the basis for discussion of possible transport scenarios and the need for further investigations at the Gnome site, not as definitive estimates of migration pathways or radionuclide concentrations.

The most critical factors affecting the transport calculations are the question of whether radionuclides from the cavity are able to move into the Culebra Dolomite, the velocity of groundwater in the Culebra, and sorption properties of the contaminants in the Culebra. To resolve these issues, the disposition of the re-entry wells drilled prior to the shot should be determined, a more rigorous determination of mean groundwater velocity should be conducted, and laboratory tests for sorption should be performed. The radionuclide source term is an additional uncertainty in the calculations presented here, and can be addressed by considering classified data in future models.



## REFERENCES

- Andricevic, R. and V. Cvetkovic, 1996. Evaluation of risk from contaminants migrating by groundwater, *Water Resources Research*, 32(3), 611-621.
- Andricevic, R., J.I. Daniels and R.L. Jacobson, 1994. Radionuclide migration using a travel time transport approach and its application in risk analysis, *Journal of Hydrology*, 163:125-145.
- Atomic Energy Commission, 1962. Plowshare Program: Project Gnome, Carlsbad, New Mexico, December 10, 1961, Final Report, Hydrologic and Geologic Studies, PNE-130F.
- Beetem, W.A. and C.G. Angelo, 1964. Tracer Study at Project Gnome Site, Near Carlsbad, New Mexico--Background Information, USGS, Technical Letter: Carlsbad Hydrology-2, Denver, CO.
- Cauffman, T.L., A.M. LaVenu and J.P. McCord, 1990. Ground-water flow modeling of the Culebra Dolomite, Volume II: Data base, INTERA Technologies, Inc., SAND89-7068/2.
- Cooper, J.B., 1962a. Ground-Water Investigations of the Project Gnome Area, Eddy and Lea Counties, New Mexico, Washington, D. C., USGS, TEI-802.
- Cooper, J.B., 1962b. Ground Water, in Atomic Energy Commission, 1962, Final Report, Hydrologic and Geologic Studies (PNE-130F), pp. 112-136.
- Cooper, J. B., 1963. Technical Letter: Carlsbad Hydrology-1, Completion and Development of USGS Test Hole 8 and USGS Test Hole 4, Carlsbad Hydrologic Studies, Eddy County, New Mexico, USGS, Denver, CO.
- Cooper, J.B. and V.M. Glanzman, 1971. Geohydrology of Project Gnome Site, Eddy County, New Mexico, Geological Survey Professional Paper 712-A, Washington, D. C..
- Dagan, G., V. Cvetkovic and A. Shapiro, 1992. A solute flux approach to transport in heterogeneous formations 1. The general approach. *Water Resources Research*, 28(5):1369-1376.
- Daniels, J.I., R. Andricevic, L. R. Anspaugh, and R. L. Jacobson. 1993, Risk-based Screening Analysis of Groundwater Contaminated by Radionuclides Introduced at the Nevada Test Site (NTS), Lawrence Livermore National Laboratory Report, UCRL-ID-112789.
- Department of Energy, 1978. Decommissioning and Decontamination Activity, Gnome Site, Eddy County, New Mexico, DOE/EA-0022.
- Department of Energy, 1982. Long-Term Hydrologic Monitoring Program, Gnome Site, Eddy County, New Mexico, NVO-241.
- Dickey, D.D. and L.M. Gard, 1962. Physical Properties, in U.S. Geological Survey, Hydrologic and Geologic Studies for Project Gnome - Final Report, PNE-130F, pp. 49-52.
- Environmental Protection Agency, 1992. Offsite Environmental Monitoring Report: Radiation Monitoring Around United States Nuclear Test Areas, Calendar Year 1991, Environmental Monitoring Systems Laboratory, Las Vegas, NV, EPA 600/R-93/141.

- Environmental Protection Agency, 1976. National Interim Primary Drinking Water Regulations, EPA-570/9-76-003, 159 p.
- Freeze, R.A. and J.A. Cherry, 1979. Groundwater. Prentice-Hall, Inc., Englewood Cliffs, New Jersey.
- Gard, L.M., Jr., 1968. Geologic Studies, Project Gnome, Eddy County, New Mexico, USGS Professional Paper 589, United States Government Printing Office, Washington, D. C.
- Gardner, M.C. and J.J. Sigalove, 1970. Evaluation of the Project Gnome/Coach Site, Carlsbad, New Mexico for Disposition, Including Identification of Restrictions, Part I, Teledyne Isotopes, Palo Alto, CA, 44 pp., AT(29-2)-1229, NVO-1229-106 Part I.
- Gelhar, L.W., 1993. Stochastic Subsurface Hydrology. Prentice Hall, Englewood Cliffs, New Jersey.
- Grove, D.B., and W.A. Beetem, 1971. Porosity and Dispersion Constant Calculations for a Fractured Carbonate Aquifer Using the Two Well Tracer Method, *Water Resources Research*, 7(1): 128-134.
- Hale, W.E., J.F. Tracy, D. Rawson, G. Coleman and N. Jaffe, 1961. Technical Papers Discussing the Effects of the Detonation on the Gnome Site, U. S. Geological Survey.
- Hoeksema, R.J. and P.K. Kitanidis, 1985. Analysis of spatial structure of properties of selected aquifers, *Water Resources Research*, vol. 21, pp. 563-572.
- Janzer, V.J., M.C. Goldberg, C.G. Angelo and W.A. Beetem, 1962. Summary of Distribution Coefficient Data for Fission Products Between Ground Water and Rocks from Project Gnome, in U.S. Geological Survey, Hydrologic and Geologic Studies for Project Gnome - Final Report, PNE-130F.
- Lappin, A.R., 1988. Summary of Site-Characterization Studies Conducted from 1983 through 1987 at the Waste Isolation Pilot Plant (WIPP) Site, Southeastern New Mexico, Sandia National Laboratories, SAND88-0157.
- Lowenstein, T.K., 1987. Post burial alteration of the Permian Rustler Formation evaporites, WIPP site, New Mexico: textural, stratigraphic, and chemical evidence, New Mexico Environmental Evaluation Group, EEG-36.
- Lynch, A.W. and R.G. Dosch, 1980. Sorption Coefficients for Radionuclides on Samples from the Water-Bearing Magenta and Culebra Members of the Rustler Formation. Sandia National Laboratories, SAND80-1064.
- Munson, D.E., A.F. Fossum and P.E. Senseny, 1989. Advances in resolution of discrepancies between predicted and measured in situ WIPP room closures, Sandia National Laboratories, SAND88-2948.

- Nathans, M.W., 1965. Project Gnome: Isotope Program - Final Report, U.S. Atomic Energy Commission, PNE-102F.
- Pearson Jr., F.J., V.A. Kelley and J.F. Pickens, 1987. Preliminary Design for a Sorbing Tracer Test in the Culebra Dolomite at the H-3 Hydropad at the Waste Isolation Pilot Plant (WIPP) Site. Sandia National Laboratories Contractor Report SAND86-7177.
- Pohll, G. and K. Pohlmann, 1996 (in press). Evaluation of the radionuclide tracer test conducted at the Project Gnome underground nuclear test site, New Mexico, Desert Research Institute Water Resources Center Publication #45126, Las Vegas, NV, DOE/NV/10845-46, UC-703.
- Pohlmann, K. and R. Andricevic, 1994. Scoping Calculations for Groundwater Transport of Tritium from the Gnome Site, New Mexico, Desert Research Institute Water Resources Center Publication #45141, Las Vegas, NV, DOE/NV/11508-08, UC-703.
- Rawson, D., C. Boardman, and N. Jaffe-Chazan, 1965. The Environment Created by a Nuclear Explosion in Salt, U.S. Atomic Energy Commission Report PNE-107F.
- Reynolds Electrical & Engineering Co., Inc., 1978. Gnome Site Decontamination and Decommissioning - Phase I Radiological Survey and Operations Report, Carlsbad, New Mexico. U.S. Department of Energy, Nevada Operations Office, NVO/0410-48.
- Reynolds Electrical and Engineering Co., Inc., 1981. Gnome Site Decontamination and Decommissioning Project, Radiation Contamination Clearance Report. U.S. Department of Energy, Nevada Operations Office, DOE/NV/00410-59.
- Smith, D.K., B.K. Esser and J.L. Thompson, 1995. Uncertainties Associated with the Definition of a Hydrologic Source Term for the Nevada Test Site. Lawrence Livermore National Laboratory, UCRL-ID-120322.
- Snyder, R.P., 1985. Dissolution of halite and gypsum, and hydration of anhydrite to gypsum, Rustler Formation, in the vicinity of the Waste Isolation Pilot Plant, southeastern New Mexico, USGS Open-File Report 85-229.
- U.S. Code of Federal Regulations, 1995, Maximum Contaminant Levels for Beta Particle and Photon Radioactivity From Man-Made Radionuclides in Community Water Systems, *in* Interim Primary Drinking Water Regulations Subpart B, Maximum Contaminant Levels. CFR Chapter 40, Part 141.16
- U. S. Department of Commerce, 1963. Maximum Permissible Body Burdens and Maximum Permissible Concentrations of Radionuclides in Air and in Water for Occupational Exposure, National Bureau of Standards Handbook 69, National Committee on Radiation Protection Report No. 22, issued in 1959 and amended in 1963.

**DISTRIBUTION**

Janet Appenzeller-Wing  
Environmental Restoration Division  
Nevada Operations Office  
U.S. Department of Energy  
P.O. Box 98518  
Las Vegas, NV 89193-8518

Bob Bangerter  
Environmental Restoration Division  
Nevada Operations Office  
U.S. Department of Energy  
P.O. Box 98518  
Las Vegas, NV 89193-8518

Joanne M. Bradbery, Director  
Contract Management Division  
Nevada Operations Office  
U.S. Department of Energy  
P.O. Box 98518  
Las Vegas, NV 89193-8518

Frank Di Sanza, Director  
Energy Technologies Division  
Nevada Operations Office  
U.S. Department of Energy  
P.O. Box 98518  
Las Vegas, NV 89193-8518

Doug Duncan  
Hydrology Program Manager  
Environmental Protection Division  
Nevada Operations Office  
U.S. Department of Energy  
P.O. Box 98518  
Las Vegas, NV 89193-8518

Virginia Glanzman  
U.S. Geological Survey  
Box 2506, MS 913  
Denver Federal Center  
Denver, CO 80225

Paul Gretsky  
International Technology Corporation  
4330 S. Valley View  
Suite 114  
Las Vegas, NV 89103

Kenneth Hoar, Director  
Environmental Protection Division  
Nevada Operations Office  
U.S. Department of Energy  
P.O. Box 98518  
Las Vegas, NV 89193-8518

Roger Jacobson  
Desert Research Institute  
Water Resources Center  
P.O. Box 19040  
Las Vegas, NV 89132-0040

Marjory Jones  
Desert Research Institute  
Water Resources Center  
P.O. Box 60220  
Reno, NV 89506-0220

Jim Kannard  
Bechtel Nevada Corporation  
P.O. Box 98521  
Las Vegas, NV 89193-8521

Randy Lacznik  
U.S. Geological Survey  
Water Resources Division  
6770 S. Paradise Rd.  
Las Vegas, NV 89119

Paul Liebendorfer  
Division of Environmental Protection  
State of Nevada  
Capitol Complex  
Carson City, NV 89710

Frank Maxwell  
Environmental Restoration Division  
Nevada Operations Office  
U.S. Department of Energy  
P.O. Box 98518  
Las Vegas, NV 89193-8518

Charles E. McWilliam, Director  
 Defense Projects Division  
 Nevada Operations Office  
 U.S. Department of Energy  
 P.O. Box 98518  
 Las Vegas, NV 89193-8518

Steve Mellington, Director  
 Environmental Restoration Division  
 Nevada Operations Office  
 U.S. Department of Energy  
 P.O. Box 98518  
 Las Vegas, NV 89193-8518

Leslie A. Monroe  
 Environmental Protection Division  
 Nevada Operations Office  
 U.S. Department of Energy  
 P.O. Box 98518  
 Las Vegas, NV 89193-8518

Peter Sanders  
 Environmental Restoration Division  
 Nevada Operations Office  
 U.S. Department of Energy  
 P.O. Box 98518  
 Las Vegas, NV 89193-8518

David K. Smith  
 Isotopes Sciences Division  
 Lawrence Livermore National Laboratory  
 P.O. Box 808, M/S L231  
 Livermore, CA 94550

Doug Trudeau  
 U.S. Geological Survey  
 Water Resources Division  
 6770 S. Paradise Rd.  
 Las Vegas, NV 89119

Annie Kelley  
 State Documents Department  
 Nevada State Library  
 Capitol Complex  
 Carson City, NV 89710

Archives  
 Getchell Library  
 University of Nevada, Reno

Beverly Carter  
 MacKay School of Mines Library  
 University of Nevada, Reno

Document Section, Library  
 University of Nevada, Las Vegas  
 4505 Maryland Parkway  
 Las Vegas, NV 89154

Library  
 Desert Research Institute  
 P.O. Box 60220  
 Reno, Nevada 89506-0220

Library  
 IT Corporation  
 4330 S. Valley View  
 Suite 114  
 Las Vegas, NV 89103  
 ATTN: Toni Miller

Library  
 Southern Nevada Science Center  
 Desert Research Institute  
 P.O. Box 19040  
 Las Vegas, NV 89132-0040

Technical Information Resource Center  
 Nevada Operations Office  
 U.S. Department of Energy  
 P.O. Box 98518  
 Las Vegas, NV 89193-8518

Public Reading Facility  
 Bechtel Nevada Corporation  
 P.O. Box 98521  
 Las Vegas, NV 89193-8521

Office of Scientific and Technical Information  
 U.S. Department of Energy  
 P.O. Box 62  
 Oak Ridge, TN 37831-9939